Valorization of solid waste products from olive oil industry as potential adsorbents for water pollution control—a review

Amit Bhatnagar, Fabio Kaczala, William Hogland, Marcia Marques, Christakis A. Paraskeva, Vagelis G. Papadakis & Mika Sillanpää

Environmental Science and Pollution Research

ISSN 0944-1344
Volume 21
Number 1

Environ Sci Pollut Res (2014) 21:268-298
DOI 10.1007/s11356-013-2135-6

Springer

Environ Sci Pollut Res (2014) 21:268–298
DOI 10.1007/s11356-013-2135-6

REVIEW ARTICLE

Valorization of solid waste products from olive oil industry as potential adsorbents for water pollution control—a review

Amit Bhatnagar · Fabio Kaczala · William Hogland · Marcia Marques · Christakis A. Paraskeva · Vagelis G. Papadakis · Mika Sillanpää

Received: 1 May 2013 / Accepted: 5 September 2013 / Published online: 26 September 2013

Abstract The global olive oil production for 2010 is estimated to be 2,881,500 metric tons. The European Union countries produce 78.5 % of the total olive oil, which stands for an average production of 2,136,000 tons. The worldwide consumption of olive oil increased of 78 % between 1990 and 2010. The increase in olive oil production implies a proportional increase in olive mill wastes. As a consequence of such increasing trend, olive mills are facing severe environmental problems due to lack of feasible and/or cost-effective solutions to olive-mill waste management. Therefore, immediate attention is required to find a proper way of management to deal with olive mill waste materials in order to minimize environmental pollution and associated health risks. One of the interesting uses of solid wastes generated from olive mills is to convert them as inexpensive adsorbents for water pollution control. In this review paper, an extensive list of adsorbents (prepared by utilizing different types of olive mill solid waste materials) from vast literature has been compiled, and their adsorption capacities for various aquatic pollutants removal are presented. Different physicochemical methods that have been used to convert olive mill solid wastes into efficient adsorbents have also been discussed. Characterization of olive-based adsorbents and adsorption mechanisms of various aquatic pollutants on these developed olive-based adsorbents have also been discussed in detail. Conclusions have been drawn from the literature reviewed, and suggestions for future research are proposed.

Keywords Olive mill · Solid waste products · Valorization · Adsorbents · Water treatment

Responsible editor: Bingcai Pan

A. Bhatnagar (✉) · F. Kaczala · W. Hogland · M. Marques
Department of Biology and Environmental Science,
Faculty of Health and Life Sciences, Linnaeus University,
391 82 Kalmar, Sweden
e-mail: amit.bhatnagar@lnu.se

A. Bhatnagar
e-mail: dr.amit10@gmail.com

M. Marques
Department of Sanitary and Environmental Engineering,
Rio de Janeiro State University, UERJ, Rio de Janeiro, Brazil

C. A. Paraskeva
Institute of Chemical Engineering Sciences, Foundation for Research and Technology, Hellas (FORTH/ICE-HT), Stadiou Street, Platani, Patras 26504, Greece

C. A. Paraskeva
Department of Chemical Engineering, University of Patras,
26504 Rion, Patras, Greece

V. G. Papadakis
Department of Environmental & Natural Resources Management,
University of Patras, 30100 Agrinio, Greece

M. Sillanpää
Faculty of Technology, Lappeenranta University of Technology,
Laboratory of Green Chemistry, Sammonkatu 12, 50130 Mikkeli,
Finland

Introduction

The increasing worldwide contamination of freshwater systems with industrial and natural chemical compounds is one of the key environmental problems (Schwarzenbach et al. 2006). About one fifth of the world's population does not have access to safe water, and two fifths suffer the consequences of unacceptable sanitary conditions (UNESCO 2003). Intensive research on effective water treatment has resulted in several technologies, which have been employed with varying degree of success for the removal of toxic pollutants from water and wastewater. Among various water treatment technologies, "adsorption" process is considered as one of the best methods available for the removal of diverse types of

pollutants from water and wastewater. Various conventional and nonconventional adsorbents have been used for their suitability towards water remediation (Bhatnagar 2012). From last few decades, research has been directed towards developing low-cost adsorbents utilizing naturally occurring and agro-industrial waste materials as these materials are cheaper, renewable, and abundantly available. Various review articles have been published in recent years where the potential of these adsorbents have been reviewed (Ahmad et al. 2012; Bhatnagar and Sillanpää 2010; 2009; Bhatnagar et al. 2010; Chuah et al. 2005; Crini 2006; Zhou and Haynes 2010). Special focus is now being given to utilize solid industrial wastes (by-products), which sometimes pose serious disposal problems. Olive oil industry is one such industry that produces enormous amount of solid and liquid wastes, and these wastes cause serious environmental problems.

Today, over 10 million ha area worldwide is covered by about 900 million olive trees, 98 % of which are located in the Mediterranean Basin (Sesli and Yeğenoğlu 2009), covering an area of 5,163,000 ha, while deriving >93 % of the total olive oil produced. The global olive oil production for 2010 is estimated to be 2,881,500 metric tons (Stamatakis 2010). The European Union countries produce the 78.5 % of total olive oil which stands for an average production of 2,136,000 tons (Stamatakis 2010). The largest olive-producing country is Spain with 1,200,000 tons followed by Italy with 540,000 tons, Greece with 348,000 tons, Portugal with 50,000 tons, and finally, France and Cyprus with 5,000 tons (Stamatakis 2010). Other non-EU-Mediterranean olive-producing countries are Tunisia with 185,000 tons, Syria with 128,000 tons, Turkey with 117,000 tons, and Morocco with 78,300 tons (IOC 2010; Niaounakis and Halvadakis 2006). Each olive tree produces 15–40 kg of olives/year depending on the climate conditions. The chemical composition of olives, which is the raw material for olive oil extraction, is very variable and depends on several factors such as, the olive variety, soil type, and climatic conditions, but in general, it consists of 18–28 % oil, 40–50 % vegetation water and stone, and 30–35 % of olive pulp (Niaounakis and Halvadakis 2006). In the last decade, olive oil production has increased by approximately 40 % worldwide. The olive tree yield is greatly affected by a biennial cycle: one year it grows, and the other year gives more fruits. Therefore, more olive oil and wastes are generated every other year (Azbar et al. 2004; Boskou 2006).

Olive oil extraction is the process of separating and collecting the oil from the olives. The main processing steps needed to obtain olive oil include: feeding, leaf removal and washing, crushing, mixing, separating the olive oil, and centrifuging the oil. Today, three different extraction processes are commonly used: (1) The traditional process, (2) the two-phase decanter process, and (3) the three-phase decanter process. In the traditional press process, the olives are washed, crushed, and kneaded with the addition of warm water (~38 °C). The resulting paste is then pressed to drain the oil, and the liquid waste originating from presses consists of a mixture of olive juice and added water and contains residual oil. Finally, olive oil is separated from the water by vertical centrifugation or decanting (Azbar et al. 2004). The use of the traditional process has decreased, and nowadays, it is almost only employed in small olive mills. The continuous system can be operated by three- and two-phase extraction technologies, diverging in the water supplies. While the two-phase system does not require the addition of water, producing olive oil and olive cake, the three-phase demands the addition of hot water to the decanter, producing olive oil, olive mill wastewater (OMW), and olive cake (residual solids). As a result of these differences, the three-phase extraction process has a slightly better yield, leading to less amount of olive cake but a significant production of olive mill wastewater (Paraskeva et al. 2007a,b; Roig et al. 2006). The traditional cold press method typically generates about 50 % of OMW, relative to the initial weight of the olives, while the continuous centrifugation process generates (80–110)% of OMW (Mantzavinos and Kalogerakis 2005). The advantages and disadvantages of each method, as well as other details, can be found elsewhere (Borja et al. 2006; Boskou 2006; Niaounakis and Halvadakis 2006).

To release most of the oil present in the olive during processing, water is used in various steps e.g., in washing, mixing (when olives are entirely dry) and diluting the paste, and in the final separation of the olive oil where the olive oil is purified. Water used in these stages corresponds to 10, 40, and 20 % out of the initial olive weight, respectively. To show the mass yield, 1 kg of olive oil is produced after the processing of approximately 5 kg of olives. The composition of the waste streams is not constant qualitatively or quantitatively, and it varies according to soil cultivation, harvesting time, degree of ripening, olive variety, climatic conditions, use of pesticides and fertilizers, and duration of aging (Niaounakis and Halvadakis 2006). In general, during the two-phase olive extraction process, olive mill waste consists of about 44 % of solid wastes and 56 % of liquid waste (Ayrilmis and Buyuksari 2010). Three-phase oil extraction procedure results in the production of ~20 % of olive oil per kilogram of treated olive fruits and both solid and liquid wastes. OMW are acidic, have extremely high biological oxygen demand (BOD) and chemical oxygen demand (COD) values (100–150 g/L), and also contain toxic levels of polyphenols (Azbar et al. 2004; Paraskeva et al. 2007a,b; Paraskeva and Diamadopoulos 2006).

According to the facts of International Olive Council, the worldwide consumption of olive oil increased of 78 % between 1990 and 2010. The increase in olive oil production implies a proportional increase in olive mill wastes. It has been estimated that the annual world olive oil production yields

enormous quantities of wastes: 8.1 million cubic meters of OMW, 3.2 million metric tons of OPC (olive press cake), and 0.3 million metric tons of leaves (Zervakis and Balis 1996). Moreover, the total amount of twigs and leaves resulting from pruning each year reaches 15 million metric tons (Nefzaoui 1995). As a consequence of such increasing trend, olive mills are facing severe environmental problems due to lack of feasible and/or cost-effective solutions to olive-mill waste management. As a matter of fact, publications related to *olive* research in indexed journals have been growing rapidly, indicating a growing interest of the scientific community on olive research (Fig. 1). The management of solid and liquid wastes in olive mills is always challenging, and extensive efforts have been made by various researchers to utilize these wastes in different beneficial products (Amar et al. 2011; Arvanitoyannis et al. 2007; Gavala et al. 2005; Georgieva and Ahring 2007; Ihemouchen et al. 2012; La Rubia-García et al. 2012; Moftah et al. 2012; Mousa et al. 2009; Paraskeva et al. 2007a; Siracusa et al. 2001). Many reviews have also been published mainly dealing with olive mill wastewater (Hamdi 1993; Hanifi and El-Hadrami 2009; Paraskeva and Diamadopoulos 2006). Besides liquid waste, solid wastes from olive mills are also of great concern, as these wastes are a source of odor nuisance, especially during warm and dry weather. These odors are attributed to volatile fatty acids, particularly butyric, caproic, valeric, and isobutyric acid (Niaounakis and Halvadakis 2006). Being a renewable resource and an industrial waste, olive mills solid wastes are, therefore, a promising resource for environmental technology if applied in the treatment of water and wastewaters. Figure 2 provides a schematic representation for the wastes generation in olive oil industry and their application as low-cost adsorbents for water pollution control.

The present review focuses on the valorization approach of different solid wastes generated in olive oil industry during olive oil production. One of the aims of this review is to provide a summary of updated information on research that has been conducted in recent years in the preparation and application of different olive mill solid wastes as adsorbents for the removal of diverse aquatic pollutants. For information pertaining to detailed experimental methodology and conditions, readers are referred to the full articles listed in the references.

Olive mill solid wastes as precursors for inexpensive adsorbents

As discussed in previous sections, the extraction of olive oil generates huge quantities of liquid and solid wastes that may have a great impact on land and water environments because of their high phytotoxicity (Roig et al. 2006) due to the presence of fats, lipids and polyphenols. Several studies have proven the harmful effects of these wastes on soil microbial populations (Paredes et al. 1987), aquatic ecosystems (DellaGreca et al. 2001), and even in air medium (Rana et al. 2003). It is, therefore, highly desirable to manage these wastes through technologies that minimize their environmental impact and lead to a sustainable use of resources. One of the interesting uses of such solid wastes is to convert them as inexpensive adsorbents for water pollution control. It provides a double-fold advantage with respect to environmental pollution. Firstly, the volume of olive mill solid waste materials could partly be reduced, and secondly, the developed low-cost adsorbents can treat industrial wastewaters at a reasonable cost. It has been suggested that the wastes from olive industry could be converted into low-cost

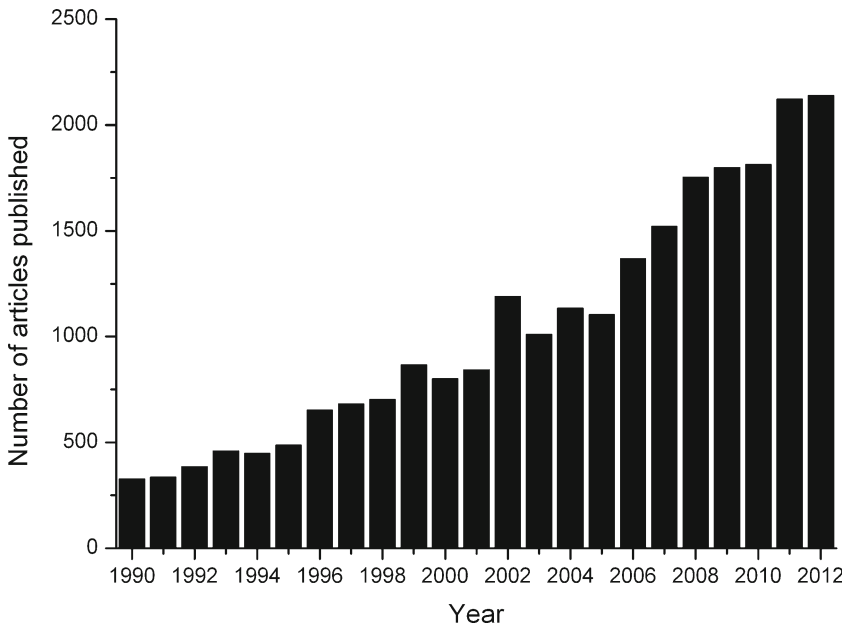

Fig. 1 Record of the number of publications in indexed journals containing the keyword "olive" between 1990 and 2012

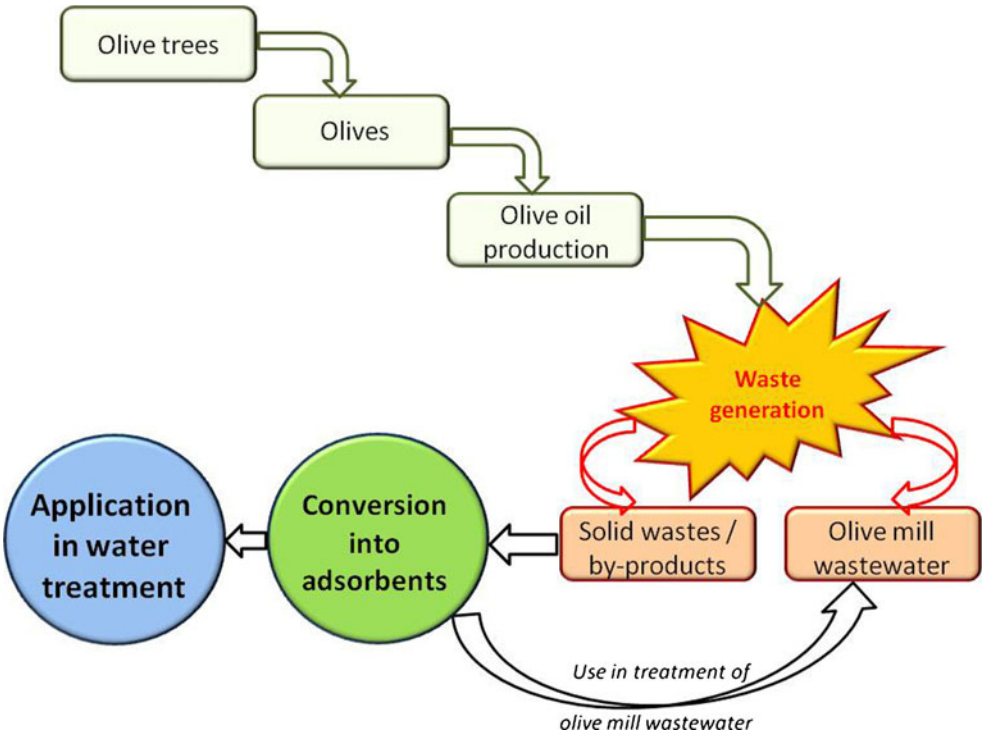

Fig. 2 A schematic representation of the wastes generated in olive oil industry, their conversion as low-cost adsorbents and their application in water pollution control

adsorbents with a cost of <$50/ton against $4,500/ton of a granular-activated carbon (Pagnanelli et al. 2003).

Various researchers have used different olive mill solid wastes by applying different physicochemical treatment methods to develop efficient adsorbents for the removal of various aquatic pollutants. The nature of the precursor, the type of activation (chemical or physical), as well as the processing conditions decides the adsorptive properties of developed adsorbents from olive wastes. In case of chemical activation, concentration of the dehydrating agent, impregnation ratio, and pyrolysis temperature govern the properties of the resulting adsorbent. A detailed description about widely used treatment methods/carbonization/activation conditions to prepare olive-based adsorbents from olive solid wastes is presented in Table 1.

Characterization of olive-based adsorbents

Different solid wastes generated during olive oil production have been characterized by different analytical techniques, and a brief discussion is presented herein. Fourier transform infrared spectroscopy (FTIR) studies revealed that olive wastes contain various functional groups such as, carboxylic, hydroxyl, methoxy, and phenolic groups that are potentially active in metals removal. This particular composition enables olive solid wastes to bind metallic ions and other pollutants in solutions and make them potential biosorbent towards water treatment applications. A detailed description about different functional groups found in the FTIR analysis of olive-based adsorbents is presented in Table 2. Energy dispersive X-ray analysis of olive mill wastes revealed the presence of potassium, calcium, sulfur, and chlorine besides carbon and oxygen (Vegliò et al. 2003). Surface area, pore volume, and adsorption efficiency towards iodine, phenol, and methylene blue are generally calculated to report the enhanced properties after chemical modifications. Table 3 represents detailed description of some of these characteristics of different olive-based adsorbents.

Application of different olive-based adsorbents in water treatment

Removal of metal ions from water and wastewater

Metal ions are one of the important categories of water pollutants, which are toxic for humans through the food-chain pyramid. Various toxic heavy metal ions discharged into the environment through different industrial activities, constituting one of the major causes of environmental pollution. Some of the important metals that have been essentially examined for their adsorptive removal using olive-based adsorbents include lead, chromium, cadmium, nickel, uranium, thorium, and mercury since these metals are present in industrial effluents and their toxicological effects are well reported in the

Table 1 Treatment methods used for the preparation of olive-based adsorbents

Raw material	Activation condition	Carbonization condition	Chemical used for treatment	Additional information	Reference
Olive cake	-	-	-	Washed with hot deionized water followed by deionized cold water; dried at 100 °C for 24 h	(Al-Anber and Matouq 2008)
Olive stone	-	-	Succinic anhydride in toluene	Washed with hot and cold distilled water and acetone, Dried at 105 °C, washed with acetone and dried (S-OS)	(Aziz et al. 2009a)
Olive stone (S-OS)	-	-	Saturated sodium bicarbonate solution	Washed with hot and cold distilled water and acetone, dried at 105 °C, washed with distilled water and acetone, finally dried	(Aziz et al. 2009a)
Olive stone	-	-	Conc. sulfuric acid (acid/olive stone ratio: 8:1, w/w)	*Before treatment*: washed with distilled water and dried at 105 °C. Treated with sulfuric acid. *After treatment*: washed with distilled water and suspended in 0.1M NaOH, refluxed for 1 h, washed and dried at 105 °C	(Aziz et al. 2009b)
Olive-waste cakes	Activated for 30–70 min at 1,023-1,123 K	Carbonized at 673 K for 1 h in N_2 flow in Prolabo stainless steel autoclave	-	Resulting material boiled in distilled water after activation for 30 min and dried at 383 K	(Baçaoui et al. 2001)
Olive waste cakes	Dried precursor mixed with H_3PO_4 solution, Activated for 2 h at 104 °C	Pyrolyzed for 2 h at 350 to 650 °C under continuous N_2 flow	Phosphoric acid	Final material washed with hot distilled water and dried at 105 °C overnight	(Baccar et al. 2009)
Olive stones	Heated at 300 °C		Treatment with 1M HCl for 8 h at 25 °C	Final materials washed with water, Dried at 100 °C for 12 h	(El Bakouri et al. 2009)
Olive stones and olive pulp	-	Heating rate: 60 °C/min; final carbonization temperature: 800 °C under vacuum (20 kN/m^2) and atmospheric pressure	-	Resulting product: Carbonized olive pulp	(Budinova et al. 2006)
Carbonized olive pulp	Activated in a water vapor stream at 800 °C for 2 h	-	-	Carbon A	(Budinova et al. 2006)
Carbonized olive pulp	Activating reagent: K_2CO_3 and H_2O, Held for 12 h, and kneaded, dried at 110 °C	Heated to 950 °C under N_2 flow at the rate of 10 °C/min for 10 min	-	Finally washed with hot water and with cold distilled water, dried at 110 °C (Carbon B)	(Budinova et al. 2006)
Carbonized olive stone	Activating reagent: K_2CO_3 and H_2O, Held for 12 h, and kneaded, dried at 110 °C	Heated to 950 °C under N_2 flow at the rate of 10 °C/min for 10 min	-	Finally washed with hot water and with cold distilled water, dried at 110 °C (Carbon C)	(Budinova et al. 2006)
Carbon A	-		-	Oxidized with 10% HNO_3 (1:3) and boiled for 1 h, Washed and dried at 105 °C (Carbon D)	(Budinova et al. 2006)
Olive cake	-	Heated to 700 °C by steps of 15 min every 100 °C, final temperature maintained at 700 °C for 1 h	-	Final material: Olive cake carbon	(Cimino et al. 2005)

Table 1 (continued)

Raw material	Activation condition	Carbonization condition	Chemical used for treatment	Additional information	Reference
Olive cake carbon	Treated with 2 N HCl for 24 h	-	-	Washed with deionized water and dried in an air oven at 80 °C overnight	(Cimino et al. 2005)
Olive cake carbon	Treated with 2 N HNO_3 for 24 h	-	-	Washed with deionized water and dried in an air oven at 80 °C overnight	(Cimino et al. 2005)
Air-dried olive cake	Treated with conc. H_2SO_4 for 12 h at 80 °C, Washed with distilled water, Soaked in $NaHCO_3$ solution followed by H_2O washing and dried at 80 °C for 6 h	Heated to 700 °C by steps of 15 min every 100 °C, final temperature maintained at 700 °C for 1 h,	-	-	(Cimino et al. 2005)
Olive bagasse	Activated under N_2 flow and steam at 750–900 °C	Carbonized at 500 °C	-	-	(Demiral 2011)
Olive pomace	-	-	-	Heated at 100–300 °C under N_2 gas flowing at 8.0 L/min	(El-Sheikh et al. 2009)
Olive cake	Mixed with conc. H_2SO_4 and heated in an oven to 200 °C for 24 h	-	Washed with distilled water and soaked in 1% $NaHCO_3$ solution	Finally washed with distilled water and dried at 105 °C for 24 h	(Fernando et al. 2009)
Olive cake	Mixed with 0.25 M NaOH for 1 h, Samples were then neutralized with HCl	-	-	Finally washed with distilled water and dried at 105 °C for 24 h	(Fernando et al. 2009)
Olive stone wastes	-	-	-	Rinsed with boiling water and cold water, dried at 105 °C	(Fiol et al. 2006)
Solvent extracted olive pulp	Activated for 1 h 30 min	Carbonized at 1,123K for 1 h 30 min, Heating rate: 10 °C/min	-	Final washing with deionized water, Dried at 110 °C (ACOP2)	(Galiatsatou et al. 2002)
Solvent extracted olive pulp	Activated for 1 h	Carbonized at 1,123K for 2 h, heating rate: 10 °C/min	-	Final washing with deionized water, Dried at 110 °C (ACOP3)	(Galiatsatou et al. 2002)
ACOP3	-	-	-	Oxidation with $(NH_4)_2S_2O_8$ in 1M H_2SO_4 in a carbon solution (1:10) at 298 K for 10 h. Final washing with deionized water, dried at 110 °C	(Galiatsatou et al. 2002)
Olive stone	Washed with 5% HCl, distilled water, Dried at 125 °C. Destructive distillation for 5 h at 600 °C under a flow of N_2, Activated by gasification with steam at 900 °C	-	-	Oxidized with $(NH_4)_2S_2O_8$, washed with distilled water and dried at 125 °C for 24 h	(Ghazy and El-Morsy 2009)
Olive stone	Treated with 1M $HCl/H_2SO_4/HNO_3/H_3PO_4$ for 24 h at room temperature	-	-	Washed with distilled water and dried at 40 °C for 24 h	(Calero de Hoces et al. 2010)
Olive stone	Mixed with 200 mL of 10%, 20% and 30% $ZnCl_2$	Heated at 650 °C in inert flow N_2 gas (150 cm^3 min^{-1} STP) for 2 h	-	Washed with 0.5 N HCl, hot water and cold distilled water, vacuum-dried at 102 °C	(Kula et al. 2008)

Table 1 (continued)

Raw material	Activation condition	Carbonization condition	Chemical used for treatment	Additional information	Reference
Olive stone	Activated with $ZnCl_2$ solution in the ratios of (starting material / activating agent) 1:1 and 1:2	Carbonized at 500–700 °C	-	-	(Kütahyalı and Eral 2010)
Olive mill solid residue	Gasified in a stream of CO_2/ air/ stream at 800–950 °C for 30–240 min	Carbonized at 800 °C for 2 h with N_2 flow of ~ 80 cm^3 min^{-1}	-	-	(Mameri et al. 2000)
Olive pomace	Mixed with 50% H_3PO_4 for 1 day	-	-	Washed with water and dried at 105 °C for 24 h	(Martín-Lara et al. 2008)
Olive pomace	Mixed with 1M H_2O_2 for 3 h	-	-	Washed with water and dried at 60 °C for 24 h	(Martín-Lara et al. 2008)
Solvent extracted olive pulp and olive stone	Activated with steam/ nitrogen mixture (flow rate: 100 mL/min, pure steam 4.5 L/h); Activation at 800 °C, heating rate 10 °C/min	Carbonized at 850 °C, heating rate: 10 °C/min, residence time: 1.5 h	-	-	(Metaxas et al. 2003)
Olive cake	Calcination at 400 °C for 1 h, Activated with KOH in a ratio KOH/C 4:1, Activated at 800 or 900 °C in 50 cc/min N_2 flow for 2–4 h	Pyrolyzed at 800 °C for 1–3 h in 50 cc/min N_2 flow	-	Final washing with HCl and water, dried at 110 °C for 24 h	(Michailof et al. 2008)
Olive wood stone/olive pulp	Activated at 800 °C with steam/N_2 mixture	Carbonized at 850 °C	-	-	(Pala et al. 2006)
Olive stone	Steam activation at 950 °C.	Carbonized at 600 °C	-	-	(Pereira et al. 2006)
Olive stone	-	Carbonized in N_2 (150 mL/ min) at 600 °C for 1 h	-	Resulting product: char	(Román et al. 2008)
Char	Activated at 800–900 °C for 20–60 min	-	Steam (0.41 g/min) diluted in N_2 (80 mL/min)	-	(Román et al. 2008)
Char	Activated at 850–900 °C for 30–120 min	-	CO_2 activation (40 mL/min)	-	(Román et al. 2008)
Char	Activated at 850 °C for 30–60 min	-	CO_2 and steam	-	(Román et al. 2008)
Char	Steam diluted N_2 flow: 80 mL/min; Activated at 850 °C; residence time: 20 min	-	-	-	(Román et al. 2008)
Olive stone	Crushed in 10% H_2SO_4, Refluxed in distilled water; Impregnated with $ZnCl_2$	Carbonized at 700 °C under N_2 flow	-	-	(Spahis et al. 2008)
Olive stone	Crushed in 10% H_2SO_4, Refluxed in distilled water; Impregnated with KOH	Carbonized at 800 °C under N_2 flow for 1 h; heating rate: 5 °C/ min	-	-	(Spahis et al. 2008)
Olive stone	Impregnated with KOH, Heated at 60 °C for 12 h and then heated at 110 °C to dryness; Pyrolyzed at 300 °C for 3 h and finally to 800 °C for 2 h in N_2 flow	Carbonized at 840 °C for 1 h in N_2 flow; heated at 10 °C/ min	Demineralized with HCl, HF	Washed with 0.1 N HCl and then with distilled water	(Ubago-Pérez et al. 2006)

Table 1 (continued)

Raw material	Activation condition	Carbonization condition	Chemical used for treatment	Additional information	Reference
Olive stone	Impregnated with $ZnCl_2$ at 70 °C, dried at 120 °C for 24 h;	Carbonized at 650 °C, under N_2 flow for 2 h	-	Washed with 0.5 N HCl, hot water, distilled water, finally vacuum-dried at 102 °C	(Uğurlu et al. 2007)
Olive stone	Treated with decalcified water and 10% H_2SO_4 for 4 h, Washed with decalcified and distilled water, Dried at 80 °C; Activated for 8 h at 900 °C in a flow of CO_2 of 120 cm^3/min.	Carbonized under flowing N_2 (100 cm^3 /min) at 400–850 °C for 2 h	-	Pre-oxidation: Heating of carbonized material to 250 °C under synthetic air (O_2/N_2) flow :100 cm^3/min for 5 h	(Wahby et al. 2011)
Olive stone	Treated with decalcified water and 10% H_2SO_4 for 4 h, Washed with decalcified water, Dried at 80 °C. Activated for 8 h at 900 °C in a flow of CO_2 of 120 cm^3/min.	Carbonized under flowing N_2 (100 cm^3 /min) at 400–850 °C for 2 h	-	-	(Wahby et al. 2011)
Olive stone	Impregnated with H_3PO_4 (60–80 wt%) at 85 °C for 4 h	Carbonized at 500 °C under N_2 flow for 2 h	-	Final washing with distilled water, oven dried at 120 °C	(Yakout and Sharaf El-Deen 2011)
Olive stone	Impregnated with H_3PO_4 (35–65 wt%) at 85 °C for 4 h	Carbonized under a flow of N_2 for 60–180 min	-	Final washing with hot water, oven dried at 110 °C	(Yavuz et al. 2010)
Olive stone	Impregnated with H_3PO_4 for 2 h; Activated at 700 °C under N_2 flow for 2 h	Carbonized in N_2 at 300 °C for 1 h	-	Soaked in 0.1 M HCl for few hours, final washing with distilled water	(Yeddou et al. 2010)

Table 2 FTIR peaks as reported in the literature for olive-based adsorbents

Material	Peak	Functional group	Reference
Olive pomace	1,704 and 1,643 cm^{-1}	C=O stretching	(Pagnanelli et al. 2003)
	1,507 cm^{-1}	C–C stretching	
Olive pomace	3,410 cm^{-1}	O–H stretching	(Pagnanelli et al. 2010)
	2,918 and 2,848 cm^{-1}	C–H stretching vibrations of CH, CH_2, and CH_3 groups	
	1,707 cm^{-1}		
	1,621 and 1,418 cm^{-1}	C=O stretching vibration of carboxylic groups	
	1,061 cm^{-1}, 1,212 cm^{-1}, and 1,136 cm^{-1}	Asymmetric and symmetric stretching of carboxylate C–O stretching vibrations of ethers and alcohols	
Waste pomace	3,409 cm^{-1}	Bonded –OH groups	(Nuhoglu and Malkoc 2009)
	2,930 cm^{-1}	Aliphatic C–H group	
	1,635 cm^{-1}	C=O stretching	
	1,507 cm^{-1}	Secondary amine group	
	1,438 cm^{-1}	Carboxyl groups	
	1,424 cm^{-1}	Carboxyl groups	
	1,317 cm^{-1}	Carboxyl groups	
	1,256 cm^{-1}	$–SO_3$ stretching	
	1,144 cm^{-1}	C–O stretching	
	1,031 cm^{-1}	C=O stretching	
	873 cm^{-1}	Aromatic –CH stretching	
	526 cm^{-1}	–C–C– group	
	465 cm^{-1}	Amine groups	
Olive stone (OS), the two-phase olive mill solid (OMS) and olive tree pruning (OTP)	3,750 and 3,050 cm^{-1}	Stretching vibration of O–H bonds into polymeric compounds, C–H stretching in aliphatic structures	(Martín-Lara et al. 2009)
	2,925 cm^{-1}, 2,855 cm^{-1}		
	1,740 cm^{-1}		
	1,650–1,635 cm^{-1}	C=O stretching	
	1,460–1,438 cm^{-1}	Carbonyl groups in different conformations such as COO^- and C=O of different organic compounds, Bending vibration of O–H bonds, Presence of aromatic rings so that double bonds (C=C) vibrations overlap the aforementioned	
	1,650–1,400 cm^{-1}		
	1,250 cm^{-1}		
	<1,500 cm^{-1}		
		C=O stretching vibration bands and O–H deformation bands, Deformation vibration of C=O of carboxylic groups, stretching vibration of OH of phenols or C–O stretching of ether groups, Stretching vibrations of C–O–C from polysaccharides	
Waste pomace	3,406 cm^{-1}	Bonded –OH groups, –NH stretching	(Malkoc et al. 2006)
	2,928 cm^{-1}	Aliphatic C–H group	
	1,635 cm^{-1}	C=O stretching	
	1,507 cm^{-1}	Secondary amine group	
	1,421 cm^{-1}	Carboxyl groups	
	1,317 cm^{-1}	Symmetric bending of CH_3	
	1,243 cm^{-1}	$–SO_3$ stretching	
	1,140 cm^{-1}	C–O stretching of ether groups	
	1,029 cm^{-1}	–C–C– group	
	873 cm^{-1}	–C–C– group	
Olive stone	3,340 cm^{-1}	–OH groups	(Calero de Hoces et al. 2010)
	2,940–2,890 cm^{-1}	Aliphatic C–H group	
	1,650 cm^{-1}	C=O stretch	
	1,590 and 1,505 cm^{-1}	Secondary amine groups	
	1,455, 1,420, and 1,365 cm^{-1}	Symmetric bending of CH_3	
	1,155 cm^{-1}	C–O stretching of ether groups	
Two phase olive mill solid (OMS) and olive stone (OS)	3,411 and 3,422 cm^{-1}	Hydroxyl peaks, Alkyl peaks	(Blázquez et al. 2010)
	2,927 and 2,925 cm^{-1}, 1,740 and 1,745 cm^{-1}	C=O bonds in carboxyl groups and their esters, Asymmetric stretching of the carboxylic C=O double bond, C–O bond in carboxylic groups, Deformation vibration of C=O carboxylic acids, stretching of the C–O–C and OH of polysaccharides	
	1,656 and 1,636 cm^{-1}		
	1,377 and 1,380 cm^{-1}		
	1,250 and 1,243 cm^{-1}		
	1,110–1,160 and 1,040–1,060 cm^{-1}		
Olive waste cake	2,929 cm^{-1}	C–H vibrations in methyl and methylene groups, Carbonyl C=O groups, Olefinic (C=C) vibrations	(Baccar et al. 2009)
	1,738 cm^{-1}		
	1,651 cm^{-1}, 1,510, and 1,425 cm^{-1}	Skeletal C=C vibrations in aromatic rings, Bands $–CH_3$ and $–CH_2^-$,	
	1,462 and 1,377 cm^{-1}		

Table 2 (continued)

Material	Peak	Functional group	Reference
	1,323 cm^{-1} 1,246 cm^{-1} 1,048 cm^{-1} 895 cm^{-1}	V (C–O) vibrations in carboxylate groups, esters (e.g., R–CO–O–R′), ethers (e.g., R–O–R′) or phenol groups, Alcohol groups (R–OH), C–H out of plane bending in benzene derivative vibrations	

literature. A brief discussion of metal ions removal by olive-based adsorbents is being presented here.

Lead

Lead [Pb(II)] in wastewater mainly comes from battery manufacturing, printing, painting, dying, and other industries. It is non-biodegradable and, therefore, must be removed from water. Lead is one of the metals that have widely been studies for its removal from aqueous solution using olive-based adsorbents. Adsorption of Pb(II) using powdered activated carbon (PACl), prepared from olive stones, has been explored by Ghazy and El-Morsy (2009). PACl was prepared in several steps, namely, washing with HCl, followed by destructive distillation and activation by gasification with steam. The modification was done by the treatment with aqueous oxidizing agent $(NH_4)_2S_2O_8$. The surface area and ash content of the PACl were reported to be 249.1 m^2/g and 5.7 %, respectively. The adsorption kinetics was found to be fast during the first stage, and adsorption occurred mainly at the surface of the adsorbent and to some extent by the internal macropores, transitional pores, and micropores. Equilibrium time of 20 min was chosen for the Pb(II) adsorption experiments. The Lagergren's pseudo-first-order model and Weber and Morris model fitted well to the experimental data and also explained the occurrence of intraparticle diffusion during the adsorption process. The effect of pH on Pb(II) removal was also investigated. It was found that Pb(II) adsorption was diminished below pH 1.0 due to the formation of oxo groups (CxO and CxO_2), which were formed on the carbon surface during activation with water and thereby hindered the Pb(II) adsorption. Complete removal of Pb(II) occurred in the pH range of 4.0–9.0 and was attributed to the adsorption of hydrolytic species, chemical interaction with the carboxylic groups of active carbon and sulfide group obtained from modification with $(NH_4)_2S_2O_8$, and/or precipitation of $Pb(OH)_2$ (s). At pH >10.0, Pb(II) removal decreased due to the incapability of adsorption of the negative species, $Pb(OH)_3^-$ and $Pb(OH)_4^{2-}$, on the negatively charged surface of PACI adsorbent. The adsorption efficiency was reported to be maximum (100 %) at PACl dosage of 60 mg/L. Increase in the number of binding sites on the adsorbent surface available to the metal ions was mainly responsible for such behavior. Increasing the temperature from 5 to 80 °C resulted in the increased efficiency of the process. This was attributed to an acceleration of some of the originally slow adsorption steps or to the creation of some new active sites on the PACl. The isotherm data was well explained by the Langmuir and Freundlich models. The procedure was applied to the removal of Pb(II) from different natural water samples and was successful enough to achieve 99–100 % recovery in distilled water, tap water, and in waters from other locations. Lead removal from potable water has also been explored using activated carbon (AC) prepared from olive stones by Spahis et al. (2008). Activated carbon was prepared by the impregnation of olive stone with $ZnCl_2$ or KOH followed by carbonization. It was observed that the AC yield decreased with activation temperature due to the loss of volatile materials. Impregnation was found to be more effective in the case of KOH as compared to $ZnCl_2$. In addition, with the increase in impregnation rate, the surface area of the ACs increased, which was attributed to the partial collapse of porosity with high impregnation rates. In addition, $ZnCl_2$ impregnation had positive effect on the development of porous texture at a relatively low pyrolysis temperature. On the other hand, treatment with KOH increased the surface area at higher temperatures. The surface area of the porous texture also increased with the rates of additives up to 14.7 mmol/g. Lead(II) biosorption using raw and chemically treated olive stones has been investigated in packed bed column (Calero de Hoces et al. 2010). Olive stone fraction <1 mm was chosen for all the tests, and the chemical modification was performed using inorganic acids (HCl, H_2SO_4, HNO_3, and H_3PO_4). Breakthrough time was found to decrease with increasing inlet Pb(II) concentration. The best results were obtained with the olive stone treated with H_2SO_4 and HNO_3. The lowest biosorption capacity was obtained for the untreated olive stone with a value of 3.81 mg/g for an inlet Pb(II) concentration of 150 mg/L. H_2SO_4-treated olive stone showed an adsorption capacity of 20 mg/g for Pb(II). The FTIR spectra of Pb(II)-loaded adsorbent suggested the involvement of –OH, –CH, and –COOH groups in the biosorption of Pb(II) ions and the possibility that biosorption could be taking place through an ion-exchange process rather than complexation. The modified

Table 3 Characteristics of olive-based adsorbents

Adsorbent	BET surface area	Micropore surface area	Micropore volume	Mesopore volume	Total pore volume	Iodine number	Methylene blue number	Reference
Treated olive stones (TOS)	–	–	–	–	–	760 mg/g	–	(Aziz et al. 2009b)
Olive-waste cakes	1,145 m^2/g	–	0.311 cm^3/g	–	–	1,390 mg/g	426 mg/g	(Baçaoui et al. 2001)
Olive waste cakes activated carbon	1,020 m^2/g	–	–	–	–	583 mg/g	312.5 mg/g	(Baccar et al. 2009)
Olive waste cakes activated carbon	793 m^2/g	–	–	–	0.49 cm^3/g	–	–	(Baccar et al. 2010)
Olive stones (raw)	324 m^2/g							(El Bakouri et al. 2009)
Thermally and chemically treated olive stones	479 m^2/g	–	–	–	–	–	–	(El Bakouri et al. 2009)
Olive stone-based AC (commercial)	587 m^2/g	–	–	–	0.333 cm^3/g	–	–	(Berrios et al. 2012)
Solvent extracted olive pulp (carbon A)	1,030 m^2/g	–	0.355 m^3/g	0.108 m^3/g	0.665 m^3/g	850 mg/g	–	(Budinova et al. 2006)
Chemically treated extracted olive pulp (carbon B)	1,850 m^2/g	–	0.461 m^3/g	0.180 m^3/g	0.898 m^3/g	1,100 mg/g	–	(Budinova et al. 2006)
Chemically treated olive stone (carbon C)	1,610 m^2/g	–	0.437 m^3/g	0.159 m^3/g	0.843 m^3/g	980 mg/g	–	(Budinova et al. 2006)
Oxidized solvent extracted olive pulp (carbon D)	732 m^2/g	–	0.315 m^3/g	0.100 m^3/g	0.645 m^3/g	488 mg/g	–	(Budinova et al. 2006)
Activated carbon from olive bagasse	523–1,106 m^2/g	357–659 m^2/g	0.1989–0.4012 cm^3/g	0.0500–0.2055 cm^3/g	0.2757–0.6067 cm^3/g	–	–	(Demiral 2011)
Partially pyrolyzed olive pomace	174–451 m^2/g	–	–	–	–	12–55 mg/g	–	(El-Sheikh et al. 2009)
H_2SO_4-activated olive cake	–	–	–	–	–	329±13 mg/g	–	(Fernando et al. 2009)
NaOH-activated olive cake	–	–	–	–	–	217±39 mg/g	–	(Fernando et al. 2009)
Olive stone waste	0.187 m^2/g	–	–	–	–	–	–	(Fiol et al. 2006)
ACOP/ACOP2/ACOP3/ACOP3ox/ ACOWS/ACOPWS	364–914 m^2/g	–	0.18–0.36 cm^3/g	0.04–0.37 cm^3/g	–	270–910 mg/g	–	(Galiatsatou et al. 2002)
Olive stone activated carbon	249.1 m^2/g	–	–	–	–	–	–	(Ghazy and El-Morsy 2009)
$ZnCl_2$-activated olive stone	58.89–790.25 m^2/g	–	–	–	–	–	–	(Kula et al. 2008)
$ZnCl_2$-activated olive stone	464.68 m^2/g	259.6 m^2/g	0.11 cm^3/g	–	–	–	–	(Kütahyalı and Eral 2010)
Activated carbon from olive mill solid residue	749–1,813 m^2/g	–	–	–	–	1,270 mg/g	–	(Mameri et al. 2000)
Carbons ACOP, ACO	364, 474 m^2/g	–	0.16 cm^3/g	0.07, 0.22 cm^3/g	–	478, 574 mg/g	–	(Metaxas et al. 2003)
Olive cake ACs	52–1,880 m^2/g	–	0.0234–0.8125 cm^3/g	0.0154–0.5531 cm^3/g	0.0388–1.1114 cm^3/g	–	–	(Michailof et al. 2008)
Powdered AC from olive wood stone, solvent extracted olive pulp	700, 800 m^2/g	–	0.19, 0.22 cm^3/g	0.12, 0.35 cm^3/g	–	–	–	(Pala et al. 2006)
Olive stone AC	855 m^2/g	–	0.36 cm^3/g	0.04 cm^3/g	–	–	–	(Pereira et al. 2006)
O.S. Carbon activated with water vapor	905 m^2/g	–	0.335 m^3/g	0.098 m^3/g	0.630 m^3/g	810 mg/g	236 mg/g	(Petrov et al. 2008)
O.S. Carbon oxidized with air	420 m^2/g	–	0.105 m^3/g	0.111 m^3/g	0.471 m^3/g	380 mg/g	158 mg/g	(Petrov et al. 2008)
Steam pyrolysis O.S. carbon	1090 m^2/g	–	0.430 m^3/g	0.110 m^3/g	0.860 m^3/g	910 mg/g	253 mg/g	(Petrov et al. 2008)
K_2CO_3 activated O.S. carbon	1610 m^2/g	–	0.437 m^3/g	0.159 m^3/g	0.843 m^3/g	1540 mg/g	394 mg/g	(Petrov et al. 2008)
SEOP Carbon activated with water vapor	1010 m^2/g	–	0.355 m^3/g	0.108 m^3/g	0.665 m^3/g	910 mg/g	356 mg/g	(Petrov et al. 2008)

Table 3 (continued)

Adsorbent	BET surface area	Micropore surface area	Micropore volume	Mesopore volume	Total pore volume	Iodine number	Methylene blue number	Reference
SEOP Carbon oxidized with air	421 m^2/g	–	0.125 m^3/g	0.115 m^3/g	0.485 m^3/g	320 mg/g	136 mg/g	(Petrov et al. 2008)
Steam pyrolysis SEOP carbon	998 m^2/g	–	0.400 m^3/g	0.060 m^3/g	0.820 m^3/g	1,050 mg/g	377 mg/g	(Petrov et al. 2008)
Carbon activated with K_2CO_3 (<0.5 mm)	1850 m^2/g	–	0.461 m^3/g	0.180 m^3/g	0.819 m^3/g	1,720 mg/g	420 mg/g	(Petrov et al. 2008)
Olive stone char	209 m^2/g	–	0.089 cm^3/g	0.016 cm^3/g	–	–	–	(Román et al. 2008)
Steam-activated olive stone	589–1,074 m^2/g	–	0.216–0.525 cm^3/g	0.042–0.124 cm^3/g	–	–	–	(Román et al. 2008)
CO_2-activated olive stone	446–778 m^2/g	–	0.243–0.406 cm^3/g	0.021–0.072 cm^3/g	–	–	–	(Román et al. 2008)
CO_2- and steam-activated olive stone	674, 1,187 m^2/g	–	0.357, 0.553 cm^3/g	0.057, 0.148 cm^3/g	–	–	–	(Román et al. 2008)
Steam/N_2-activated olive stone	589, 713 m^2/g	–	0.358, 0.312 cm^3/g	0.042, 0.091 cm^3/g	–	–	–	(Román et al. 2008)
$ZnCl_2$ olive stone (0.5–1 mm)	501–856 m^2/g	–	0.196–0.288 mL/g	–	–	–	–	(Spahis et al. 2008)
KOH-activated olive stone	831–1,541 m^2/g	–	0.326–0.604 mL/g	–	–	–	–	(Spahis et al. 2008)
KOH-activated olive stone	–	–	0.19–0.41 cm^3/g	–	0.21–0.44 cm^3/g	–	–	(Ubago–Pérez et al. 2006)
Activated olive stone	58.89–790.25 m^2/g	–	–	–	–	–	–	(Uğurlu et al. 2007)
Olive stone ACs (preoxidized)	1,212–1,410 m^2/g	–	0.49–0.57 cm^3/g	0.03–0.04 cm^3/g	–	–	–	(Wahby et al. 2011)
Olive stone ACs (conventional activation)	953–1,591 m^2/g	–	0.38–0.62 cm^3/g	0.02–0.13 cm^3/g	–	–	–	(Wahby et al. 2011)
H_3PO_4-activated olive stone	257–1,218 m^2/g	–	0.11–0.5 cc/g	0.012–0.1 cc/g	0.123–0.6 cc/g	–	–	(Yakout and Sharaf El–Deen 2011)
H_3PO_4-activated olive stone	525.20–1,740.0 m^2/g	–	0.2254–0.7520 cm^3/g	0.0346–0.3316 cm^3/g	0.2600–0.9088 cm^3/g	–	–	(Yavuz et al. 2010)
Olive stone ACs (AC–OS)	680 m^2/g	–	–	–	–	420 mg/g	–	(Yeddou et al. 2010)

olive adsorbent exhibited negative charge over the entire range of investigated pH, but the untreated olive stone was found to be possessing positively charged groups below pH 5.0.

Blázquez et al. (2010) studied the biosorption of lead using olive stone (OS) and two-phase olive mill solid (OMS). OMS is a semisolid mixture of pulp and olive stones obtained from the crushing of olives, which yield the oil in a two-phase decanter system. It contains around 55–60 % moisture, has a dark color, and forms a sludge-like mass. The maximum adsorption capacities for Pb(II) ranged between 6.39–5.25 and 23.7–23.1 mg/g for OS and OMS, respectively, with the increase in temperature from 25 to 60 °C. The equilibrium data obtained from the adsorption experiments was analyzed in the light of adsorption models, viz., Langmuir, Freundlich, Sips (for OS), and a two-step Langmuir-type model and an adaptation of the Dubinin–Astakov model (for OMS). The Langmuir isotherm fitted well to the experimental data of OS and OMS. The mechanism of Pb(II) uptake by OS and OMS was also elucidated with the help of FTIR analyses. The spectra of both the adsorbents were similar and hence confirmed the presence of similar functional groups on the surface of the adsorbents. Peaks for hydroxyl, and alkyl groups were seen in the spectra of OS and OMS. Peaks attributing to the presence of C–O bond, C=O double bond were also present in the spectra of the two adsorbents. Changes in the FTIR spectra were observed after Pb(II) biosorption, which exhibited the involvement of the functional groups in the adsorption process. The efficiency of OS, the two-phase OMS and olive tree pruning (OTP) for Pb(II) removal from aqueous solutions has been reported (Martín-Lara et al. 2009). The three solids were milled and <1.000 mm fraction was chosen for the biosorption tests. The elemental analysis of the three biosorbents was found to be similar. The adsorbents OS and OTP exhibited low water content (10 %) and OMS had high water content (>50 %) and a considerable fat content (>4 %) due to its way of obtaining. The potentiometric titration results suggested that OMS was richer in active sites than OTP and OS. The calculated titration curves of discrete and continuous models were compared with the experimental data, and it was observed that continuous model fitted well to experimental data. The pH_{pzc} values showed that all adsorbents had an acidic surface. The heterogeneous nature of the three adsorbents was confirmed by their IR spectra. The Langmuir model fitted well to the Pb(II) isotherm data obtained at pH 5.0. The maximum metal uptake capacities obtained with OS, OMS, and OTP were 0.031, 0.122, and 0.110 mmol/g, respectively. The presence of soluble organic compounds in the three adsorbents was also detected with higher concentration in OMS and OTP (700 and 450 mg/L mean values, respectively) than OS (47 mg/L).

Optimization studies for the removal of Pb(II) from aqueous solutions using different olive mill wastes (OS, two-phase OMS, and OTP) have also performed (Martín-Lara et al. 2011). Two 32 full factorial designs were performed to identify important factors and their interactions. Validation of the statistical model was carried out by taking 14 g/L and pH 5.0 in the validation experiments. Under the given conditions, OS, OMS, and OTP removed 78.10, 85.00, and 95.20 % Pb(II), which was in agreement with the predicted values (81.14, 90.02, and 98.61 % for OS, OMS, and OTP, respectively) suggested by the models. Initial metal concentration in the solution affected the biosorption capacity of the adsorbents, and an increase in metal concentration lowered the metal uptake capacity due to the saturation of the active sites on the adsorbents. Temperature variation between 25 and 60 °C did not influence on the metal uptake capacity. The response surface plots well exhibited the interactions between main variables and their effects on the responses.

Olive tree pruning waste was also examined for the removal of Pb(II) from water (Blázquez et al. 2011b). Removal of Pb(II) was studied at pH 5 in a batch system. The pseudo-first-order, pseudo-second-order, and Weber and Morris kinetic models were applied to test the kinetic experimental data. The pseudo-second-order kinetic model provided the best correlation of the experimental data, indicating that adsorption might be the rate limiting step for Pb(II) biosorption by olive tree pruning waste. Equilibrium experimental results were fitted to Langmuir, Freundlich, and Sips model isotherms to obtain the characteristic parameters of each model. The Langmuir and Sips isotherms best represented the measured biosorption data. According to the Sips model calculation, the maximum biosorption capacities of olive tree pruning wastes for Pb(II) were found to be 26.24, 33.39, and 32.15 mg/g at 25, 40, and 60 °C, respectively.

Chromium

Chromium, another important metal, has many industrial applications such as in textile, electroplating, leather tanning, and metallurgy industries, and therefore, the wastes generated by these industries are rich in hexavalent Cr(VI) or trivalent Cr(III) forms of chromium. The removal of Cr(III) by olive stone activated carbon was investigated by Pereira et al. (2006). The Brunauer, Emmett, and Teller (BET) surface area of the adsorbent was found to be 855 m^2/g with micro- and mesopore volume of 0.36 and 0.04 cm^3/g, respectively. The concentrations of carboxylic and phenolic groups in the adsorbent were reported as 0.057 and 0.34 mmol/g, respectively. The presence of surface groups suggested that metal removal might have occurred due to the surface complex formation and exchange between metal ions and acidic functional groups. The pH of point of zero charge (pH_{pzc}) of the adsorbent was observed between 2.0 and 3.0. A flow rate of 2 mL/min was found to be optimum for the studies as it promoted a higher average residence time, which allowed favorable mass transfer parameters. A favorable isotherm with a pronounced plateau at

0.45 meq/g was obtained. Lower amount of superficial sites for adsorption was attributed to the lower Cr(III) uptake by the adsorbent. The equilibrium data fitted well to the Langmuir model. Intraparticle diffusion was considered to be the rate controlling step for the adsorption process. In an another study, researchers used olive stone waste for Cr(III) removal (Blázquez et al. 2011a). The elemental analysis of the olive stone showed the presence of C (52.34 %), H (7.11 %), N (0.03 %), and S (<0.1 %). Titration and IR analysis revealed the predominance of carboxylic groups in olive stone and were considered to be mainly responsible for chromium removal. Packed bed column studies were also undertaken to investigate the feasibility of the process at pilot scale. The breakthrough time was found to increase with increasing bed height, which was attributed to the increase in number of binding sites broadening the mass transfer zone. Higher Cr(III) uptake was observed at highest bed height due to the increased biosorbent dosage, which provided more binding sites for adsorption, although the adsorption capacity in the continuous system (0.913 mg/g) was found to be lower as compared to that found in batch studies (5.185 mg/g).

Hexavalent chromium [Cr(VI)] is more toxic than Cr(III) and, therefore, pose serious environmental concern. In an attempt to remove Cr(VI), activated carbon, produced from olive stones, was chemically activated using sulfuric acid (OS-S) and utilized as an adsorbent (Attia et al. 2010). Adsorption results obtained for activated carbon (OS-S) were compared with acid-treated commercial activated carbon (CAC-S). The optimum pH for Cr(VI) uptake was found to be 1.5. The equilibrium adsorption data was better fitted to the Langmuir model. The results of kinetic models showed that the pseudo-first-order kinetic model was found to correlate the experimental data well. It was concluded that activated carbon produced from olive stones (OS-S) had an efficient adsorption capacity compared to (CAC-S) sample. The waste pomace of olive oil factory (WPOOF) has also been investigated for its adsorption properties for the removal of Cr(VI) in batch and fixed-bed column (Malkoc et al. 2006). The WPOOF included olive (6–8 %), water (20–33 %), and seeds and pulps (59–74 %) depending on the olive oil extraction processes. The desired range of particle sizes (1.0–3.3 and 0.15–0.25 mm) of the adsorbent were obtained by grinding. The FTIR spectra of WPOOF, before and after adsorption, exhibited that the bonded –OH groups and/or –NH stretching and carboxyl groups played a major role in Cr(VI) biosorption. Maximum Cr(VI) adsorption occurred at pH 2.0 (8.4 mg/g) but was reduced (2.7 mg/g) when the solution pH was increased. The lowering of adsorption capacity at high pH was attributed to the increase in H^+ ion concentration and increase in overall charge on the adsorbent surface, which caused hindrance in the adsorption of negatively charged Cr ions like $Cr_2O_7^{2-}$, and CrO_4^{2-}. It was proposed that Cr(VI) removal by the biomass occurred by two mechanisms: direct reduction of Cr(VI) to Cr(III) by contact with the electron-donor groups of the biomass and indirect reduction including binding of Cr(VI) to the positively charged groups on the biomass surface followed by the reduction of Cr(VI) to Cr(III) by adjacent electron donor groups and, finally, the release of Cr(III) ions into aqueous solution due to electronic repulsion between the positively charged groups and the Cr(III) ions. With increase in initial Cr(VI) concentration from 50 to 200 mg/L, uptake capacity of WPOOF increased from 6.1 to 12.15 mg/g. Higher availability of Cr(VI) ions in the solution resulted in the increase in uptake capacity of pomace. In addition, the higher initial Cr(VI) concentration increased driving force to overcome all mass transfer resistance of metal ions between the aqueous and solid phases resulting in higher probability of collision between Cr(VI) ions and adsorbents. The rise in temperature also affected the Cr(VI) uptake and was attributed to the fact that bond rupture of functional groups took place on adsorbent surface at high temperature resulting in an increase in active adsorption sites. Langmuir model provided a better fit to the Cr(VI) adsorption onto pomace adsorbent. In case of column studies, the flow rate also strongly influenced the Cr(VI) removal and adsorption capacities of 3.33, 1.17, and 0.96 mg/g at 5, 10, and 20 mL/min, respectively, were recorded. The breakthrough curve became steeper when the flow rate was increased with which the adsorbed Cr(VI) ion concentration decreased. It was attributed to the short residence time of the solute in the column. Maximum values of total adsorbed Cr(VI) quantity, maximum Cr(VI) uptake, and Cr(VI) removal percentage were reported as 78.26 mg, 3.33 mg/g, and 21.74 %, respectively, at 5 mL/min flow rate. The data from the column studies fitted well to the Adams-Bohart model.

Cadmium

Cadmium and its compounds have been found extremely toxic even in low concentrations and bioaccumulate in organisms and ecosystems. The removal of Cd(II) has been examined by olive-based adsorbents by different researchers. Kula et al. (2008) assessed the potential of activated carbon prepared from olive stone (ACOS) for the removal of Cd(II) from aqueous solutions. $ZnCl_2$ was selected for chemical activation with different amounts. The impregnation was conducted at 70 °C and then dried at 120 °C. Two hundred milliliters of 10, 20 and 30 % $ZnCl_2$ were used to mix olive stone samples denoted as $ACOS_1$, $ACOS_2$, and $ACOS_3$, respectively. After carbonization and washing, the samples were vacuum dried. The ACOS adsorbent was differentiated on the basis of their *w*/*w* % of $ZnCl_2$ impregnation, particles size, and other physicochemical properties. The activated carbons having activation with 20 % $ZnCl_2$ ($ACOS_2$) showed the maximum BET surface area (790 m^2/g). The scanning electron micrograph (SEM) image of the ACOS confirmed the presence of pores of

different size and shapes. The external surface of the chemically activated carbon was found to be full of cavities and was attributed to the evaporation of $ZnCl_2$ during carbonization. The adsorption of $ACOS_2$ was found to be four times higher than that of raw olive stone (~80–20 %). The adsorbent dosage for the experiments was set as 1.0 g/50 mL. The absolute amount of Cd(II) per unit of adsorbent increased from 0.68 mg/g to 1.654 mg/g at 303.15 K with the increase in metal ion concentration from 15 to 45 mg/L. The adsorption of Cd(II) onto $ACOS_2$ was found to increase with the increase in pH. At alkaline pH (>9.0), a decreasing trend in uptake was observed due to the formation of soluble hydroxyl complexes. Temperature elevation in the adsorption system did not favor Cd(II) adsorption onto $ACOS_2$, which showed that the physical adsorption governed the adsorption mechanism. The kinetic data fitted well to the pseudo-second-order model and intraparticle diffusion model. The isotherm data was well explained by both the Langmuir and the Freundlich models. In an attempt to improve the performance of olive stone wastes as adsorbent, succinylated-olive stone (S-OS) adsorbent was prepared by the esterification of lignocellulosic matrix of olive stone waste with succinic anhydride in heterogeneous conditions and tested for Cd(II) removal from aqueous solutions (Aziz et al. 2009a). The FTIR spectra provided unequivocal evidence for efficient esterification of the adsorbent. MAS ^{13}C NMR spectroscopy also confirmed the occurrence of succinylation reaction. Titration results showed a total concentration of carboxylic functions (nCOOH) value of 3.9 mequiv/g for the olive adsorbent exhibiting that esterification functionally modified the olive waste. The kinetics of adsorption process of Cd(II) onto sodium treated S-OS (NaS-OS) was rapid with 99 % adsorption occurring within the first 15 min of contact time. The readily accessible adsorption sites, which were abundant and strong ionic interactions between the succinate groups anchored at the surface of the material and cadmium ions in solution, were found responsible for the fast kinetics. Adsorption mechanism was found to be governed by chemical adsorption via ion exchange between the adsorbate and adsorbent. The Langmuir isotherm fitted well to the experimental data confirming the homogeneous distribution of active succinate linkers on the surface of the adsorbent. The NaS-OS material exhibited a maximum uptake capacity of 200 mg/g for Cd(II), but the adsorbed Cd(II) onto NaS-OS was found lower than the succinate groups' content. The steric crowding of Cd(II) due to the larger hydrated radius of the ion (8.52 Å) was found to induce a quick saturation of adsorption sites caused by the linker and accentuated by the free rotation of ethylene carbons in succinate groups, which eventually lowered the Cd(II) adsorption capacity. Desorption performance of 88–92 % for Cd(II) was obtained over five repeated adsorption–desorption cycles confirming the reusability of the modified olive waste.

Batch adsorption studies for the removal of Cd(II) from aqueous solution using olive cake as adsorbent have also been reported (Al-Anber and Matouq 2008). The Cd(II) removal efficiency was found to increase when the solution pH was increased from 2.0 to 6.0, although a decrease in Cd(II) adsorption was observed when the solution pH further increased from 6.0 to 11.0. The removal efficiency was found to be 66 % at pH 6.0 at 28 °C. The increase in the cadmium ions removal with increase in pH from 2.0 to 6.0 was attributed to the decrease in H^+ ions concentration with the pH increase. At higher pH (pH 6.0), the surface of the olive cake became increasingly negatively charged attracting the positive charge ions to attach to the free binding sites, whereas H^+ ions would not compete with cadmium ions for the adsorption sites on olive cake. On the other hand, the decrease in the adsorption rate with the increase in pH from 6.0 to 11.0 was attributed to the formation of $Cd(OH)_3$, taking place as a result of dissolution of $Cd(OH)_2$. Based on the speciation diagram, it was reported that all the species occurring at pH 8.0 and below carry a positive charge either as Cd^{2+} or $Cd(OH)^+$, which also explained that the H^+–Cd^{2+} exchange reaction governed the adsorption mechanisms of Cd(II). Removal efficiency of Cd(II) by olive cake adsorbent decreased with the increase in solution temperature from 28 to 45 °C. This observation had been attributed to the relative increase in the escaping tendency of the Cd(II) ions from the solid to the bulk phase and deactivation of the adsorbent surface or destruction of some active sites on the adsorbent surface due to bond ruptures. It might also be due to the weakness of adsorptive forces between the active sites of the adsorbents and the adsorbate species and also between the adjacent molecules of adsorbed phase. The higher dose of adsorbent in the solution also resulted in increase in the removal efficiency of Cd(II) from aqueous solution due to the greater availability of exchangeable sites for the ions. Results showed that with an increase in temperature from 28 to 45 °C, the maximum adsorption capacity decreased from 65.4 to 44.4 mg/g. The thermodynamic calculation for the adsorption of Cd(II) by olive cake adsorbent revealed that the process was feasible and exothermic.

Zinc

Zinc, in small concentrations, is an essential element for living organisms and plants. On the other hand, when concentration of zinc increases above a limit, it becomes toxic to humans, animals, and plants. The main sources of zinc to the environment are mining operations, secondary metal production, coal combustion, rubber tire wear, and phosphate fertilizers. The removal of Zn(II) by olive-based adsorbents has also been examined by various researchers. Waste olive cake (OC) has been utilized for Zn(II) removal from wastewaters by Fernando et al. (2009). The characterization results showed

that OC fractions >2 mm (chemically or nonchemically treated) had lower iodine numbers and thus lower surface area than materials without fractionation resulting in materials with poorer characteristics for adsorption of low-molar-mass solutes. The nonfractionated material was comprised of different sized particles. The results also indicated that chemically treated OCs presented higher iodine numbers than nonchemically treated ones. Chemical activation with H_2SO_4 resulted in OCs with higher surface area and degree of microporosity as compared to the treatment with NaOH. Nonfractionated material had higher nitrogen and mineral content than fractionated material (>2 mm fractions). Chemically treated materials also presented lower mineral content, which was due to the removal of inorganic matter by the chemical treatment. The nonfractionated materials were used for studying the effect of contact time on Zn(II) adsorption. Under identical conditions, OC-NaOH and the waste olive cake exhibited higher removal efficiency for Zn(II) than the OC-H_2SO_4. The lower adsorption efficiency shown by OC-H_2SO_4 was attributed to the competition between high concentrations of H^+ released by the biosorbent surface and the metal ions in solution. Kinetic data fitted well with the pseudo-second-order model, and the modeling results also suggested that the rate-limiting step in the biosorption systems might have been chemisorption involving valence forces through sharing or exchange of electrons between adsorbent and metal. The pH studies showed that amount of zinc ions adsorbed by the adsorbents increased sharply with the increase in pH from 3.0 to 4.5–5.0 and then increased more slowly with the increase in pH from 4.5–5.0 to 6.0. After pH 6.0–7.0, the amount of zinc uptake remained constant. It has also been confirmed by literature that Zn^{2+} is mostly present in solution in its divalent ionic form, with smaller amounts in the form of $ZnOH^+$ at pH>6.0, making it favorable for biosorption in an increasingly negatively charged surface. At lower pH, a competition between H^+ and Zn^{2+} ion species exists for the sites of adsorption, due to the high H^+ concentration, while at higher pH this effect was diminished. The amount of Zn(II) ions adsorbed per unit mass of adsorbent increased with the increase in initial zinc concentrations. It was attributed to the decrease in pore diffusivity with increasing initial metal concentration. Zn(II) adsorption on the adsorbents was attributed to adsorption processes on the particle surface, mainly those related to ion exchange or surface complex formation. The maximum adsorption capacity obtained from the Langmuir isotherms was found in the range of 14–27 mg/g for different studied adsorbents prepared from OC.

Zinc removal from aqueous solutions was studied using AC produced from solvent extracted olive pulp (SEOP) (Galiatsatou et al. 2002). The other raw materials like olive, peach, and apricot stone were also used to produce activated carbon in the study. Carbonization of the materials was performed at 1123 K in N_2 atmosphere, and the adsorbents were named ACOP (AC from SEOP), ACO (AC from olive), ACP (AC from peach), and ACA (AC from apricot stone). The materials were further activated using steam/nitrogen mixture at 1073 K. ACOP2 and ACOP3 were prepared by carbonization for 1 h 30 min and 2 h, respectively. In this way, products of different burn-off levels and different ash contents were produced. Carbon ACOP3ox was prepared by oxidation of ACOP3. ACOPWS, and ACOWS carbons were obtained by treating ACOP and ACO with H_2SO_4. The N_2 adsorption isotherms of the prepared activated carbons revealed high degree of microporosity along with the mesoporosity. The ACO favored mesoporosity, while SEOP resulted in higher macropore volume. Carbon ACOP2 had higher volume in the whole pore range and more developed surface area as compared to ACOP3, and this was consistent with their time of activation. Significantly lower gasification levels and a decrease in mesopore (more profound for ACOWS) and macropore volume were observed in ACOWS and ACOPWS. Iodine number was not much affected showing that the removal of the inorganic matter mainly influenced the larger pores. Oxidation of ACOP3 carbon lowered the iodine number, due to the presence of acidic groups, which block the pore entrances of micropores. All carbons were basic in nature except ACOP3ox, which was acidic, and ACOWS and ACOPWS, which were neutral. It was observed that the equilibrium was reached within 10 h for Zn^{2+} with ACOP. ACOP carbon showed significantly higher removal ability for Zn^{2+}, than the other carbons reaching almost 100 % of the initial concentration, even in concentrated solutions [8.6×10^{-4} M $Zn(NO_3)_2$]. Despite the difference in surface area and pore volume (micro- to macropores), carbons ACOP2 and ACOP3 possessed similar amounts of surface groups and showed similar adsorption levels for zinc ion. The ACOP3ox exhibited lower adsorption maxima as compared to ACOP3 at unadjusted pH. Carbons ACO and ACA, prepared under similar experimental conditions, reached similar levels of adsorption, but had different degree of inorganic matter. Carbon ACP showed minimum adsorption of Zn^{2+}. It was also found that the untreated SEOP carbons were of low oxygen content, <0.8 mmol [O]/g. Hence, the basicity of the carbons used was due to their ability to form electron-donor acceptor complex. Alike other studies of metal adsorption by olive adsorbents, at lower pH, a competition between H^+ and Zn^{2+} ion species for the sites of adsorption occurred due to the high H^+ concentration, while at higher pH, the effect was diminished.

Zinc removal from the effluents discharged from the industries has also been investigated using untreated olive mill solid wastes as adsorbent (Hawari et al. 2009). The equilibrium was reached in 60 min for the initial concentration of 0.25 mmol/L Zn(II) and 180 min for the 1–3 mmol/L initial concentration of Zn(II). It was observed that Zn(II) adsorption decreased onto olive mill residue with the increase in the particle size due to

the decrease in surface area. Thus, particle sizes ranging from 0.85 to 1.18 mm were used in the study. Maximum adsorption capacity for Zn(II) occurred at pH 5.0 with the initial zinc concentration of 4 mmol/L, olive mill residue concentration of 20 g/L, at room temperature, and a particle size ranging from 0.84 to 1.18 mm. In acidic medium (pH<2.0), the Zn(II) adsorption was low due to the competition between H^+ ions and Zn(II) ions for the adsorption sites. On the other hand, at pH 6.0, the metal ion precipitated. The olive adsorbent concentration was also critical for the process, and it was reported that with an increase in adsorbent dose from 1 to 100 g/L, Zn(II) removal increased from 27 to 95 %, but the amount of zinc ions adsorbed per unit mass decreased from 0.4 to 0.01 mmol/g. It might be due to the aggregation of the adsorbent particle, which could have decreased the surface area of the adsorbent. An adsorbent dose of 4 g/L was found to be adequate for Zn(II) removal. The maximum adsorption capacity for Zn(II) by olive adsorbent was reported as 5.63, 6.46, and 7.11 mg/g (0.188, 0.216, and 0.237 mmol/g) at 298, 308, and 328 K, respectively. Results from the study confirmed that the adsorption process was endothermic in nature and an increase in adsorption efficiency at higher temperature was attributed to the bond rupture of functional groups on adsorbent surface increasing the number of active adsorption sites, thus enhancing adsorption. The increase in adsorption capacity with an increase in temperature implied chemisorption. The Langmuir model fitted well to the isotherm data, and pseudo-second-order provided the best fit to the kinetics of the process.

Copper

Copper ions can be found in many wastewater sources including printed circuit board manufacturing, electronics plating, plating, wire drawing, copper polishing, paint manufacturing, wood preservative using, and printing operations. High concentration of copper compounds in drinking and agriculture water sources may cause adverse effects.

The removal of Cu(II) using exhausted olive waste cakes chemically activated by phosphoric acid have been investigated by Baccar et al. (2009). A concentration of 60 % H_3PO_4 was found to be the most suitable for the development of a high specific surface area of the adsorbent material. Maximum adsorbent porosity was achieved with pyrolysis temperature of 450 °C. The iodine number, which indicates the microporosity of an adsorbent, was highest at an impregnation ratio of 1.75. The weight ratio of the resulting adsorbent was found to be 42.9 %. The FTIR analysis of the prepared adsorbent revealed the presence of carbonyl, esters, and alcohol groups on the surface. A more carbonaceous and aromatic structure of adsorbent due to the dehydration effect of acid and evolution of volatiles during pyrolysis was formed. IR and chemical analysis also suggested that phosphoric acid chemical activation led to the incorporation of phosphorous in the structure of the obtained adsorbent. Further on, introduction of weakly acidic functional groups through surface oxidation using $KMnO_4$ was carried out which resulted in insoluble MnO_2 on the adsorbent surface. The adsorption of Cu(II) on olive cake was investigated by potentiometry at pH 6.0, I= 0.1 M $NaClO_4$, 25 °C, and under atmospheric conditions (Konstantinou et al. 2007). Numerical analysis of the experimental data supported the formation of surface complexes and allowed the evaluation of the corresponding formation constant, which was found to amount log β=5.1±0.4. This value was close to corresponding values given in literature for Cu(II)–humate complexes, indicating that the same type of active sites (e.g., carboxylic and phenolic groups) was responsible for the Cu(II) binding by olive cake. Addition of a competing metal ion [e.g., Eu(III) ion] in the system led to replacement of the Cu(II) by Eu(III). Evaluation of the potentiometric data obtained from competition experiments indicated that ion exchange was the main mechanism that took place in the system. The formation constant of the Eu(III) species adsorbed on olive cake was found to be log β=5.4±0.9.

Nickel

The major sources of nickel contamination to water comes from industrial process such as electroplating, batteries manufacturing, mining, and metal finishing. The removal of nickel [Ni(II)] from aqueous solution using activated carbon prepared from olive stone impregnated with $ZnCl_2$ has been reported (Uğurlu et al. 2009). The adsorption kinetics was found to be rapid for the first 30–35 min, and equilibrium was achieved in 150 min. It was observed that percent removal of Ni(II) increased with an increase in pH from 3.0 to 6.0, remained constant between 6.0 and 8.0, and decreased in pH>8.0. Experiments were conducted with 15 mg/L Ni (II) concentration with solid/liquid of 1 g/50 mL, temperature of 303 K, and time of 1.5 h. Optimum uptake of Ni(II) was observed between pH 6.0 and 8.0 (96.0 %). The Ni(II) adsorption was found to decrease with the rise in temperature (293–313 K) due to the tendency of Ni(II) to escape from the solid phase to the bulk phase. Pseudo-second-order model described the adsorption kinetics satisfactorily. The adsorption of Ni(II) from synthetic wastewater has also been investigated using waste pomace of olive oil factory (Nuhoglu and Malkoc 2009). The BET surface area and bulk density of the pomace adsorbent were 1.24 m^2/g and 0.509 g/cm^3, respectively. Particle size of 0.15–0.25 mm was used for the adsorption study. With an increase in dosage from 5.0 to 15.0 g/L, an increase in adsorption of Ni(II) from 58.9 to 80 % was observed. The adsorption per unit mass was noted to decease with rising adsorbent dosage (from 11.78 to 5.33 mg/g), which was attributed to the overlapping

and aggregation of adsorption sites. The adsorption removal efficiency was affected by stirring speed, and it was found that on increasing the speed from 180 to 480 rpm, the removal of Ni(II) ion increased from 61.3 to 81.2 % and adsorption capacity increased from 6.13 to 8.12 mg/g. Maximum adsorption was found around pH 4.0, and a decrease in adsorption was observed below and above it. Enhanced competition of proton with Ni(II) ions for the binding sites and complex formation resulted to the decreased Ni(II) adsorption at low pHs. At pH >4.0, the Ni(II) ions gets precipitated due to hydroxide anions forming a nickel hydroxide precipitate, which was a reason for decreased adsorption at higher pH values. The FTIR spectra of the raw and modified adsorbent showed the presence of the functional groups, viz., aliphatic, secondary amine, carboxyl, and amine groups, which were responsible for the Ni(II) adsorption. Langmuir model fitted well to the experimental isotherm data and the kinetics was well explained by the pseudo-second-order model. The monolayer adsorption capacity of the adsorbent for Ni(II) was found to be 14.80 mg/g.

Mercury

Mercury is a hazardous environmental contaminant. The anthropogenic emission sources of mercury mostly result from solid waste incineration (municipal and medical wastes), coal and oil combustion, pyrometallurgical processes (iron, lead, and zinc), and production of mercury and gold (Pirrone et al. 1996; Wang et al. 2004). The removal of mercury cations, Hg(II) from aqueous solutions using activated carbon prepared from olive stones has been reported by Wahby et al. (2011). Physical activation and a pre-oxidation treatment method were used for the modification of the olive stone. Carbonization was done at 400, 550, 700, and 850 °C. The activation was performed by heating the sample at 900 °C for 8 h. The optimum preoxidation temperature was found to be 250 °C. The preoxidized (at 850 °C) olive stone activated carbon exhibited the maximum Hg(II) removal (72 %). It was found that introduction of surface oxygen groups such as carboxyl, phenol, and lactone by the preoxidation treatment favored the Hg(II) adsorption onto the prepared AC. As compared to other metals, less reports for Hg(II) adsorption by olive-based adsorbents are available in literature.

Iron

The adsorption of Fe(III) ions from the aqueous solution using olive cake as an adsorbent has also been investigated (Al-Anber and Al-Anber 2008). Maximum removal efficiency of Fe(III) was achieved at pH 4.5 over a range of temperatures (28–45 °C). At lower pHs, binding sites of Fe(III) became positively charged due to high proton concentrations that competed with metal cations resulting in lower uptake rates of Fe(III). With the increase in pH from 2.0 to 4.5, the concentration of proton decreased in the solution and did not compete with Fe(III) for the adsorption sites on olive cake thus facilitated greater Fe(III) uptake. Insoluble iron hydroxide precipitation from the solution was shown to be responsible for decreased removal efficiency above pH 4.5. Increase in adsorbent dose resulted in higher removal efficiency of Fe(III). The experimental results were well described by Langmuir, Freundlich, and Dubinin–Kaganer–Radushkevich (D-K-R) isotherm models and pseudo-second-order kinetic model. Some other researchers have also examined the potential of olive-based adsorbents for iron removal (Hodaifa et al. 2013; Nieto et al. 2010).

Arsenic

Arsenic toxicity is well known, and many reports and articles have been published reporting the toxic nature of arsenic and its compounds. Budinova et al. (2006) prepared activated carbons obtained from olive waste materials for arsenic(III) removal. The carbonization of olive material was conducted at 800 °C. The obtained carbon from extracted olive pulp was activated in a water vapor stream at 800 °C. The precursors (solvent extracted olive pulp and olive stones) were then activated with activating reagent, K_2CO_3 and water and then dried. Afterwards, the sample was carbonized at 950 °C, washed with hot water, and finally with distilled water and then dried. The steam treated carbon (carbon A) was further oxidized with HNO_3 to obtain carbon with great number of oxides. The proximate analysis of raw materials showed that olive stones and olive pulp had relatively low ash and sulfur contents, which were desirable for activated carbon production. C/H and C/O atomic ratios of the olive pulp were found considerably higher than those of the olive stones. The chemical composition of the raw materials was found to be different and affected the properties and the adsorption capacity of the obtained carbons. The method of treatment and the raw material composition were seen to influence the composition of obtained carbon. Solvent extracted olive pulp and olive stones by chemical activation with K_2CO_3 resulted in increased content of micropores and high surface area. The results showed that chemical activation provided better As(III) adsorption results in comparison to adsorbents obtained by steam activation and steam–HNO_3 oxidation. The probability for catalytic influence of all carbons on the oxidation of As(III) to As(V) was also investigated in this study. It was concluded that the catalytic influence of the activated carbons was from 30 to 10 % for the carbons with alkaline character of the surface and from 50 to 12 % for the carbon with acidic character of the surface in the range of concentrations of 5–20 mg/L As(III). The removal of As(III) increased with time

and attained equilibrium in 60 min. The adsorption capacity for arsenic ions of the activated carbon prepared after pyrolysis in a vacuum by water vapor activation, carbons obtained from chemical activation of extracted olive pulp and olive stones with K_2CO_3 were 18.60, 11.42, and 9.85 μmol/g, respectively. Maximum As(III) adsorption was found at pH 7.9 and showed a sharp decrease below and above 7.9.

Removal of different metals from single and binary aqueous solution

Olive-based adsorbents have also been used for the removal of different metals from single and binary aqueous solution. Biosorption of different metals (cadmium, chromium, and lead) has been investigated using olive stone adsorbent (Hernáinz et al. 2008). Milled stones obtained with a 1-mm sieve separator were used for the study. For the three metals, it was observed that for Cd(II), metal precipitation occurred at pH>9.0, for Cr(III), at near-neutral value (6.0–8.0), and for Pb(II), metal precipitation occurred at pH>6.0. Cd(II) removal efficiency was found to increase from 45 to 82 % when the solution pH was increased from pH 3.0 to 9.0. Whereas, in case of Cr(III), maximum removal (86.0–90.2 %) took place in the pH range of 4.0–6.0. Maximum removal (75.6–87.8 %) of Pb(II) occurred at pH 4.0–6.0 using olive stone adsorbent. The adsorption experiments were conducted at pH ≤7.0 to avoid precipitation. The adsorption kinetics was fast for the three metals as >60 % of metal adsorption occurred in first 15 min, and 120 min was chosen as the equilibrium time for the isotherm experiments. The kinetics of the three metals was able to suggest that the metal binding occurred preferably on the solid surface with no significant ion diffusion toward the inside of the particle. The biosorption of Cd(II), Cr(III), and Pb(II) onto olive stone followed the pseudo-second-order kinetic model. The increase in temperature from 25 to 40 °C resulted in the increased adsorption of Cd(II) and Pb(II) onto olive stone sorbent but the Cr(III) adsorption was found to decrease at higher temperature, which was attributed to the damage of active binding sites in the biomass at higher temperature. Sips model fitted well to the isotherm data and showed that maximum adsorption capacity by olive stone of the three metals was in the order of Cr(III)>Cd(II)>Pb(II). The use of olive stones as adsorbents for the removal of Cr(VI) and Cd(II) from aqueous solutions has also been studied (Rouibah et al. 2009). Adsorbent with the particle size <0.314 mm was used for the adsorption studies. Kinetics of Cr(VI) was found to be fast with about 80.44 % removal in first 5 min, and equilibrium was attained in 30 min with a removal of 99.77 %. The kinetics of Cd(II) onto olive stone adsorbent was slower, and it took 120 min to reach equilibrium with an adsorption capacity of 3.21 mg/g corresponding to 68.88 % Cd(II) removal. The Cr(VI) removal was found maximum (99.77 %) at pH 2.0, which was attributed to the presence of $HCrO_4^-$ at low pHs, which induces an electrostatic attraction between the adsorbent surface and the anions. The increase in pH lowers the surface protonation and results in other forms of chromium (CrO_4^{2-} and $Cr_2O_7^{2-}$) causing a decrease in adsorption. The effect of pH was not very prominent in case of Cd(II). The cadmium adsorption was found to increase from 26.14 to 68.88 % with the rise in temperature from 5 to 22 °C. Although when temperature was further increased to 40 and 50 °C, Cd(II) adsorption declined due to the desorption of some of the cadmium ions from inside the pores back into the solution. Even Cr(VI) adsorption increased with the rise in temperature and remained constant at temperature >40 °C. The Cr(VI) adsorption onto olive stone adsorbent was fitted well to the Langmuir model, whereas both Langmuir and Freundlich models well explained the Cd(II) adsorption process. The pseudo-second-order kinetic model satisfactorily explained the adsorption kinetics of both the metals.

In an another study, the removal of Cd(II) and Cr(VI) from aqueous solutions has been examined (Rouibah et al. 2010). The equilibrium adsorption capacity of the olive stones for Cr(VI) followed the Langmuir model, whereas for the Cd(II) cation, the two models, Langmuir and Freundlich, could be equally representative. The adsorption process was found to be of pseudo-second order. It was reported that the olive stones retained chromium more than cadmium, but at optimal conditions, high removal percentages were reached for both metals. Another study was carried out for the removal of different heavy metals, namely, (Pb(II), Ni(II), Cu(II), and Cd(II)) from single and binary aqueous solutions using olive stone waste separated from pulp generated in the oil production industry (Fiol et al. 2006). The cation-exchange capacity (CEC) of olive stone waste and the release of K^+, Mg^{2+}, and Ca^{2+} from acid-washed olive stone waste was determined. The total ionic content was found to be 0.304 meq/g dry wastes (0.019, 0.025, and 0.261 meq/g of K^+, Mg^{2+}, and Ca^{2+}, respectively). Specific surface area and bulk density of 0.187 m^2/g and 1.25 mg/cm^3 was reported for the olive stone waste. The material composition was 49.38 % C, 0.17 % N, and 6.08 % H. The adsorption kinetics was completed in 1 h, and maximum removal of metals occurred in the first 20 min. The process followed the pseudo-second-order rate equation, suggesting that the biosorption might be the rate-limiting step involving valence forces through sharing or exchange of electrons between adsorbent and adsorbate. High metal removal occurred in the pH range of 4.0–7.0. At lower pH, the adsorption was negligible, which was explained by the fact that the proton concentration increased at acidic pH, which lead to the competition between metal cations and protons for the surface sites. Adsorption isotherm data for single component system were described by Langmuir and Freundlich isotherm models. The best fit was provided by Freundlich model for all the studied metals adsorption on olive stone

waste. Binary metals mixture removal was also studied at pH 5.5 using equimolar metal concentrations. The uptake values calculated for each metal in binary system varied slightly from the Langmuir model value. The metal removal by olive stone waste was affected by the presence of NaCl and $NaClO_4$ salts. Even at low salt concentration (0.1 mol/L), 70 % decrease in metal uptake occurred except in case of Cu removal. In comparison to $NaClO_4$, NaCl exerted a slight greater influence on metal removal, which was attributed to the presence of competing Na^+ ions for metal binding. A significant release of Ca^{2+}, Mg^{2+}, and K^+ from olive stones was also found during the uptake of Cd, Pb, Ni, and Cu. Furthermore, higher Ca^{2+} was released proving that it was the major cation in the olive stone matrix. The exchange of cations showed that the ion exchange was also responsible for the cation uptake by the adsorbent. The highest desorption percentage was obtained for Pb (68 %) when the highest HCl concentration (0.1 mol/L) was used. In similar conditions, 57.2, 49.2, and 33.1 % desorption of Cu, Cd, and Ni, respectively, were obtained.

The olive mill solid residue was pressed, sun dried, grounded and used for the metal uptake studies (Pagnanelli et al. 2002). The kinetics of copper, zinc, and cadmium were found to take place within 2 h, whereas, for mercury and lead, 4 h was required to attain equilibrium. For the Cu biosorption experiments, the pomace was treated with distilled water or n-hexane. The use of n-hexane reduced the organic release in the treated effluent, but at the same time, metal uptake was diminished in comparison to the water prewashed material. Moreover, water pretreatment was found sufficient to reduce COD release in the effluent according to the law limit. Biosorption phenomenon was assumed to occur by a general ion exchange mechanism combined with a specific complexation reaction for copper ions. The regeneration studies confirmed the affinity of the biosorbent for lead as compared to that for cadmium. The Cd and Pb uptake after regeneration was found to be 56 and 81 %, respectively.

Removal of selected heavy metals, namely, cadmium(II), lead(II), nickel(II), zinc(II), and chromium(III) from aqueous solutions using solid residue of olive mill products (SROOMP) was studied (Gharaibeh et al. 1998a). The presence of adsorbed zinc and lead on the SROOMP was confirmed by XRF spectra, and the concentrations of the metals were 0.57 and 1.76 % by weight, respectively. Olive pomace has also been used as an adsorbent to investigate its adsorption efficiency for heavy metals (copper and cadmium ions) (Martín-Lara et al. 2008). Olive pomace (OP) was treated with H_3PO_4 (PAOP) and H_2O_2 (HPOP). Copper adsorption was best obtained by using PAOP (0.090 mmol/g) in comparison to HPOP (0.056 mmol/g) or untreated olive pomace (0.043 mmol/g). Increasing concentration of activating agents or longer activation time did not improve the copper adsorption. The results from the potentiometric titration showed that PAOP was richer in active sites than OP and HPOP due to the oxidation that increased acidic sites concentration. In addition, HPOP had decreased acid site concentration due to the partial degradation of the vegetal matrix in comparison to the untreated pomace. Titration modeling denoted that all investigated biosorbents (OP, PAOP, and HPOP) were characterized by the same kinds of active sites (carboxylic and phenolic), but with different total concentrations with PAOP richer than OP and HPOP. The isotherm data was analyzed using Langmuir model, which provided a reasonable fitting to the data. Chemical treatment of the adsorbent showed an increase in adsorption capacity for the two metals with PAOP exhibiting the highest adsorption for either metal. Copper adsorption was found to be greater than cadmium adsorption at similar pH for the three studied adsorbents, which was attributed to the atomic weight of cadmium (cadmium is about two times heavier than copper) due to which cadmium presents a larger sterical impediment than copper at charge parity. The presence of $NaNO_3$ also affected the metal adsorption onto the modified adsorbents. The order of decrease in copper uptake in the presence of sodium was, PAOP>HPOP>OP, while for cadmium, the order was, HPOP>OP>PAOP.

Pyrolysis, another process that has been widely used for the preparation of activated carbon, has also been used for preparing OP-based adsorbents and to develop a preconcentration procedure for the metal ions (El-Sheikh et al. 2009). Heat pretreatment at low temperature (100–300 °C) under inert atmosphere was done to prepare the adsorbents. The characterization results showed that the total acidity decreased with the increase in pyrolysis temperature, while the total basicity generally increased. No systematic trend in the values of methylene blue and iodine number was observed with the temperature of pyrolysis. OP-200 (OP pyrolyzed at 200 °C) and OP-150 (OP pyrolyzed at 150 °C) provided the highest value for methylene blue and iodine numbers, respectively. The prepared adsorbents were used for the adsorption of Cu^{2+}, Cd^{2+}, and Zn^{2+}. The results exhibited that the adsorption capacity of Cu^{2+} was negatively influenced by the pretreatment of olive adsorbent. On the other hand, the highest adsorption capacity for Zn^{2+} and Cd^{2+} was obtained with OP-150. The preconcentration of metals was also studied during the study. It was observed that with raw OP, 85–-97 % recovery of Cu^{2+}, Cd^{2+}, and Zn^{2+} was possible at pH 5.0, but the loading flow rate of water (flow rate between 0.3 and 0.4 mL/min) was too slow, making the use of raw OP impractical. In the case of heat-treated OP adsorbents, the metal recovery and adsorbent permeability (flow rate of water sample) were the parameters used for choosing the best pyrolyzed adsorbent. Highest recovery towards Cu^{2+} was achieved using OP-100 and OP-150 (100 and 97 %, respectively) at pH 5.0. OP-150, 100, and 200 showed good results for Cd(II) removal (98, 93, and 87 %, respectively)). All pyrolyzed adsorbents performed well in case of Zn^{2+} recovery at pH 5.0. The presence of relatively

high amount of total acidic groups was a reason for the recovery values obtained for OP-100, OP-150, and OP-200. Permeability of raw OP was found to be very low (flow rate was between 0.3 and 0.4 mL/min at various pH values) and pressure reduction caused cartridge reduction. The permeability of partially pyrolyzed OPs was comparatively better than the raw counterpart. The permeability was in the order: OP-300>OP-200>OP- 250>OP-150>OP-100. OP-200 was finally selected as the preconcentrating adsorbent (pH of water sample, 5.0; sample flow rate, 4.3 mL/min). High preconcetration levels of metals were ensured by optimizing the parameters: eluent concentration and volume, mass of adsorbent, and volume of water sample. Nitric acid was used as the eluent due to its strong ability to dissolve metals. Maximum amount of the adsorbed metal ions was eluted by 5 mL of 0.50 M HNO_3. The effect of interfering ions was investigated. Analytical performance of the method was also done, and satisfactory correlation coefficients were obtained in the range of 0.996–0.973. The validation of the method was checked and was found that the method had credibility and gave comparable results just similar to the results obtained from the analysis by "electro-thermal vaporization atomic absorption spectrometer." Simultaneous determination of Cu^{2+}, Cd^{2+}, and Zn^{2+} in complex water samples was found to be possible by the proposed method.

Lead and zinc adsorption was examined onto exhausted olive pomace ash (EOPA) from aqueous solution (Elouear et al. 2009). Kinetic studies showed that an equilibrium time of 2 h was required for the adsorption of Pb(II) and Zn(II) onto EOPA. Equilibrium adsorption was affected by the initial pH (pH_0) of the solution. pH_0=6.0 was found to be optimum for individual removal of Pb(II) and Zn(II) ions by EOPA. Adsorption tests of EOPA in synthetic wastewater revealed that the adsorption data of this material for Pb(II) and Zn(II) ions were better fitted to the Langmuir isotherm based on correlation coefficients. Monolayer adsorption capacities of EOPA were 8.76 and 7.75 mg/g for Pb(II) and Zn(II), respectively. Olive mill solid residue was used for the removal of different heavy metals (Hg, Pb, Cu, Zn, and Cd) (Lucey 2002). The effect of pretreatments by water and n-hexane and the regeneration possibility was also examined. Olive mill solid residue was able to remove heavy metals from aqueous solutions with an affinity series reflecting not only the hydrolytic properties of the metallic ions but also a particular affinity for copper. It was supposed that biosorption phenomenon occurred by a general ion exchange mechanism combined with a specific complexation reaction for copper ions. Water pretreatment was sufficient to reduce COD release in the effluent according to the law limit, while n-hexane pretreatment strongly reduced also the adsorption properties of this material. Adsorption isotherms obtained under different operating conditions were fitted using a non linear regression method for the estimation of the Langmuir parameters. Moreover a simple Scatchard plot analysis was performed for a preliminary investigation of the active sites, showing the presence of two different site affinities depending on the metal concentration, according to the previous hypothesis of two kinds of uptake mechanisms for copper biosorption. Regeneration tests provided good results in terms of yield of regeneration and also concentration ratios.

The adsorption potential of dried olive oil husks (SW001) for zinc and copper ions has also been reported (Al-Asheh and Banat 2001). Freundlich and Langmuir isotherms described the adsorption of Cu^{2+} and Zn^{2+} ions reasonably well. Upto 90 % of Zn^{2+} ions and 80 % of Cu^{2+} ions were adsorbed from aqueous solutions when the initial adsorbent and metal concentrations were 30 and 20 mg/L, respectively. An increase in the SW001 concentration resulted in higher metal removal from the aqueous solution, and an increase in Zn^{2+} ion or Cu^{2+} ion concentration at constant SW001 concentration increased the metal loading per unit weight of the adsorbent. An increase in the initial pH of the metal solutions enhanced the SW001 adsorption potential. The uptake of Zn^{2+} ions was also enhanced by decreasing the SW001 particle size. The presence of a high concentration of soft ions (Na^{+}) strongly suppressed the uptake of Zn^{2+} ions by SW001. The removal characteristics of Cd(II) and Ni(II) ions from aqueous solution by exhausted olive cake ash (EOCA) were investigated (Elouear et al. 2008). Batch kinetic studies showed that an equilibrium time of 2 h was required for the adsorption of Ni(II) and Cd(II) onto EOCA. Equilibrium adsorption was found to be affected by the initial pH (pH_0) of the solution. The pH_0 6.0 was found to be the optimum for the removal of Cd(II) and Ni(II) ions by EOCA. The adsorption test with EOCA for synthetic wastewater revealed that the adsorption data of this material for nickel and cadmium ions were better fitted to the Langmuir isotherm since the correlation coefficients for the Langmuir isotherm were higher than that for the Freundlich isotherm. The maximum uptake capacity of EOCA for nickel and cadmium ions was 8.38 and 7.32 mg/g, respectively. The adsorption ability of ground, sieved and washed olive tree pruning waste (OPW) obtained as twigs from various olive cultivated region of Turkey was investigated for the removal of Cu(II), Cd(II), and Pb(II) from aqueous systems (Uzunosmanoglu et al. 2011). Adsorption was found to be strongly dependent on pH, contact time, initial concentration of the heavy metal ions, and adsorbent dosage. The highest value of Langmuir maximum uptake was found for copper followed by cadmium and lead.

The olive mill waste (OMW) from the two-decanter olive-oil-production system has also been used as biosorbent for different heavy metals removal (Martinez-Garcia et al. 2006). The characterization results of OMW suggested the presence of a high calorific value of the dry matter in OMW although it had high moisture content hindering its use as a fuel. The OMW also consisted of high phosphate and organic levels.

The average OMW particle size was 50–200 μm. The SEM micrograph of the OMW exhibited the heterogeneous nature of the waste (the pulp of the fruit and fragments of olive stones mixed together). Maximum efficiency (75 % removal) of the OMW biosorbent was exhibited for Pb(II), whereas minimum removal occurred in the case of aluminum. The adsorption capacities of the heavy metals studied in this study were in the order of: Pb>Cd>Cu>Hg>Fe>Al. The agitation speed to obtain satisfactory metal removal was set at 150 rpm, which avoided the fragmentation of biomass. Acidic pH (<3.0) was not favorable for metal adsorption and also at pH higher than 8.0, metal uptake capacity decreased. It was observed that Pb and Cd adsorption increased at pH 4.0 and reached maximum at pH 6.0 and 7.0 for Cd and Pb, respectively. Copper adsorption was found to decrease in presence of other metal ions. Fe and Cd showed synergistic adsorption effects in mixed solutions. In trimetallic solutions, the biomass efficiency was found to reduce due to the saturation of the available binding sites. The OMW was found to maintain its adsorptive capacity over 10 cycles.

Adsorption properties of olive husk were investigated under equilibrium (batch tests) and dynamic (column tests) conditions for removing heavy metals from aqueous streams (Volpe et al. 2003). Husk samples were contacted with aqueous solutions of nitric salts of Pb, Cd, Cu, and Zn at 25 °C. Adsorption isotherms obtained from equilibrium data were fitted and interpreted by the Freundlich model. Metal-saturated husk samples resulting from column tests were air-dried and incinerated to simulate combustion in order to assess the fate of sorbed metals. The results demonstrated that, under both equilibrium and dynamic conditions, metal sorption capacity of the husk was in the sequence Pb>Cd>Cu>Zn. For all the metals, calculated Freundlich constants decreased by increasing initial metal concentration or decreasing solution pH. In dynamic tests, a significant reduction of sorption capacity was recorded (except for copper) when a metal was fed simultaneously to the others: Pb (77 %), Cd (93 %), and Zn (68 %). Combustion tests carried out on metal-saturated husk samples showed that the average losses of lead and cadmium, as volatile species, were always three to four times greater than the losses of copper and zinc, in both single- and multimetal-saturated samples.

The use of activated carbon prepared from olive stones for the removal of radionuclides such as uranium and thorium from aqueous solutions has also been investigated (Kütahyalı and Eral 2010). Chemical activation of the starting material was done using $ZnCl_2$ as chemical agent. The carbonization was done at varying temperatures (500–700 °C). All activated carbons used in this study had a particle size of <0.125 mm. In case of uranium, adsorption capacities were reported to be very similar for all types of adsorbents. However, in the case of thorium, 500 °C carbonization temperature and starting material/activating agent ratio of 1:2 provided the highest adsorption capacity. The maximum adsorption capacities of the adsorbent were found to be 0.171 and 0.087 mmol/g for uranium and thorium, respectively. The BET surface area of the adsorbent was found to be 464.68 m^2/g. The micropore volume and area were reported as 0.11 cm^3/g and 259.6 m^2/g, respectively. The kinetics was fast and 5 and 30 min were chosen as shaking times for uranium and thorium, respectively. The kinetic data fitted well to the pseudo-second-order model. The uranyl ions formed very stable complexes with carbonate around pH 7.0, and the adsorption decreased above pH 6.0 due to the formation of $[UO_2(CO_3)_2]^{2-}$ and/or $[UO_2(CO_3)_3]^{4-}$. In case of thorium, pH 4.0 was optimum for achieving maximum adsorption. At pH 4.0 and 5.0, complexes like $[ThCH_3COO]^3$, $[Th(CH_3COO)_2]^{2+}$ and $[Th(CH_3COO)_2]^{2+}$, and $[Th(CH_3COO)_3]^{+}$, respectively, dominated. An increase in the initial metal ion concentration from 25 to 300 mg/L, lead to an increase in the adsorption capacity of activated carbon from 6.1 to 52.2 mg/g for uranium and 4.5–18.3 mg/g for thorium. The uptake of uranium and thorium increased slightly with increasing temperature. The Langmuir model explained well the uranium adsorption, whereas the thorium isotherm data was well fitted to the Freundlich model.

The effectiveness of the uranium removal by olive cake from aqueous solutions was demonstrated in batch experiments (Konstantinou and Pashalidis 2007). The adsorption capacity was evaluated by using both Langmuir and Freundlich isotherms. The optimum pH for uranium adsorption on olive cake was 7.5. The amount of adsorbed uranium was governed by the amount of active sites on the biomass surface indicating an inner sphere complexation. The adsorption of uranium on olive cake was endothermic and entropy-driven process and did not depend on the ionic strength of the solution. The removal of radiotoxic Th^{4+} from aqueous solutions was also explored using two activated carbons prepared from solvent extracted olive pulp (SEOP) and olive stone (OS) by a two-step physical activation method with some other adsorbents (Metaxas et al. 2003). The activated carbon prepared from SEOP was termed ACOP, and the one obtained from olive stone was named ACO. ACO carbon had a higher surface area, more developed micropore and mesopore volume, but lower macropore volume than ACOP carbon. The selectivity of the ACOP towards the radioactive element was more as compared to the ACO. Langmuir model best described the isotherm data of the ACOP and ACO and the adsorption capacity of ACOP for thorium was more than ACO.

Removal of mixed pollutants from single and binary aqueous solution

The removal of metal ion (cadmium) and a dye (safranine) has also been studied (Aziz et al. 2009b) using treated olive stones

(TOS). Olive stones were treated with concentrated sulfuric acid at room temperature followed by subsequent neutralization with 0.1 M NaOH. The chemical treatment resulted in a highly porous material with pores of different shapes and sizes. Cavities in external surface suggested the high surface area of the TOS material. The iodine number value (760 mg/g) also confirmed the high surface area of TOS. Treatment of TOS with sulfuric acid resulted in its high sulfur content due to the known sulfonation of lignocellulosic constituents of the olive stone leading to the formation of sulfonic acid functional groups. The TOS exhibited adsorption capacities of 128.2 and 526.3 mg/g for cadmium and safranine, respectively. Low value of pH_{pzc} (2.6) for TOS resulted in cadmium and safranine uptake in the pH range of 3.0–6.0 and 4.0–10.0, respectively. Due to the constant pH range for adsorption of the two pollutants, the ion exchange was suggested as the responsible adsorption mechanism. The adsorbed amounts of safranine and cadmium were 1.49 and 1.14 mmol/g, respectively. The cadmium species present in aqueous solution at pH 4.0 were Cd^{2+}, $Cd(OH)^{+}$, and $Cd(HCO_3)^{+}$. The higher uptake of safranine dye was attributed to an additional adsorption by a hydrophobic interaction process between the TOS surface and the organic dye molecules. Adsorption behavior of carbons prepared from olive cake was tested for the adsorption of several wastewater pollutants (Cimino et al. 2005). Different forms of olive cake carbon (OCC) were produced by carbonization of the olive cake at 700 °C and further treatment with different chemicals such as, HCl, HNO_3, and H_2SO_4 and respective forms of OCC were prepared. The adsorption of heavy metals (HM) (Ag^{+}, Cd^{2+}, Cr^{3+}) that were different for both the ionic charge and the radius of hydrated ion was tested. Ph (phenolic compound), MB (dyeing compound), and dodecylbenzenesulfonic acid–sodium salt detergent (DBSNa, anionic surfactant) were other pollutants studied. The adsorption studies revealed that the contact time required to reach equilibrium was minimum for heavy metals and maximum for Ph and MB (1 h for HM, 6 h for DBSNa, and 16 h for both Ph and MB). The OCC and H_2SO_4 showed a basic property (pH_{pzc}: 9.20 and 9.95, respectively), whereas OCC-HCl and OCC-HNO_3 were acidic in nature (pH_{pzc}, 2.96 and 2.83, respectively). The ash content and the water content and acid losses of the acid washed OCCs were found to be reduced as compared to OCCs. The increase in acidity of OCC-HCl and OCC-HNO_3 was attributed to the removal of inorganic oxides (Al, Fe, K, Ca, Mg, and S) and to the protonation of basic sites on carbon surface. The sulfation of the OCC-H_2SO_4 was confirmed by the high content of both ash and sulfur in it. The scanning electron microscopy (SEM) images of OCC and treated derivatives were distinct and cavities were clearly visible in the H_2SO_4-OCC. Cadmium removal decreased with increasing ionic strength of medium (NaCl or $NaNO_3$ as background electrolyte). Similar trend was also observed with Ag^{+} and Cr^{3+}. In case of MB removal, the H_2SO_4-OCC showed poor performance as compared to the other adsorbents (OCC-HCl, OCC-HNO_3, H_2SO_4-OCC, F 200, CC). When compared to commercial carbons, the olive cake carbon exhibited good adsorption capacity for Ph and HM based on sorption affinity values (K^*). Removal of MB and DBSNa compounds by OCC was slightly lower than that observed for commercial activated carbons. In multiple pollutant removal using OCC derivatives, a high removal of Cd (66 %) in presence of the two other heavy metals (Ag^{+} and Cr^{3+}) occurred. It was also observed that Cd(II) removal increased to 78 and 98 % in the presence of Ph and DBSNa, respectively. More effective adsorption of cadmium ions in the presence of chromium ions occurred and was attributed to the presence of new adsorption sites, which were generated from the adsorption of Cr^{3+} on the carbon surface (the monomeric and dimeric ionic forms). The overall results suggested that the treatment of olive cake with acid increased their adsorption efficiency to a great extent.

Removal of organic pollutants from water and wastewater

Dyes

Dyes are important aquatic pollutants, which are generally present in the effluents of textile, leather, paper, and dye manufacturing industries. The worldwide high level of production and extensive use of dyes generates colored wastewaters and these effluents are generally considered to be highly toxic to the aquatic biota. Thus, the removal of dyes from effluents before they are mixed up with unpolluted natural water bodies is important. Olive-based adsorbents have been employed as adsorbents to remove different classes of dye from water and wastewater. Activated carbon (AC) prepared from olive stone has been used for the adsorption of CI reactive red 22 dye from aqueous solution (Uğurlu et al. 2007). The maximum surface area of the AC (790.25 m^2/g) was achieved by applying chemical treatment with 20 % *w*/*w* $ZnCl_2$. The external surface of chemically activated carbon was full of cavities and was porous in nature as compared to the raw adsorbent, suggesting that the evaporation of $ZnCl_2$ during carbonization was the reason behind the porous nature of the AC. The dye adsorption became constant in 120 min and up to 78 % color removal occurred with the adsorbent dose of 4 g/200 mL. The adsorption of dye decreased with the increase in pH due to the change in surface charge of the adsorbent. Higher adsorption under acidic conditions might be related to the preference of the dye ions for active sites and/or increase in accessibility to interlayer regions of protonated and monomeric species. The kinetics and the isotherm data of the dye onto AC was satisfactorily explained by the pseudo-second-order model and Langmuir model, respectively. A study was undertaken to compare the ability of activated carbon prepared from olive stone (ACOS) with that of

commercial AC for reactive red 22 dye adsorption (Uğurlu et al. 2008). The kinetics was found to be completed in 60 min for both the adsorbents and maximum removal for the ACOS and AC were 60 and 80 %, respectively. The pseudo-second-order kinetic model for the adsorption of dye onto AC and ACOS fitted well with the data. The isotherm was satisfactorily explained by the Langmuir model for both the adsorbents.

Olive-stone-based activated carbon has also been exploited for the adsorption of methylene blue (MB) dye from wastewater (Berrios et al. 2012). The equilibrium and kinetics of adsorption were examined at temperatures ranging from 25 to 40 °C and at different agitation speeds. The equilibrium and kinetics data for MB adsorption showed a good fit to the Freundlich model and first-order reaction. The MB adsorption decreased onto the olive-stone AC with the increase in temperature. As the MB molecule has a minimum molecular diameter of 0.8 nm and cannot enter pores with a diameter of <1.3 nm; thus, it only enters the larger micropores and mostly gets adsorbed in the mesopores. This explained that despite the high surface area of olive stone-based AC (587 m^2/g), the adsorption capacity of MB in aqueous solution (0.858 mg/g at 25 °C with an AC dose of 0.5 g/L) was poor due to the molecular diameter of MB and the AC pore size distribution. Activated carbon was prepared from olive bagasse by chemical activation with phosphoric acid, and the prepared activated carbon was used to remove methylene blue from aqueous solutions (Demiral 2011). The surface area and total pore volume of chemically modified activated carbon were 936 m^2/g and 0.598 cm^3/g, respectively. The effects of various experimental parameters, such as pH, contact time, temperature, and the amounts of adsorbent, were investigated in batch adsorption. The experimental data indicated that the adsorption isotherms were well described by the Langmuir equilibrium isotherm. The maximum adsorption capacities onto activated carbon at 25, 35, and 45 °C were found to be 71.43, 73.53, and 88.49 mg/g, respectively. The pseudo-first-order, pseudo-second-order, and intraparticle diffusion models were used to describe the kinetic data, and the rate constants were evaluated. The experimental data fitted very well to pseudo-second-order kinetic model. A combination of olive pomace after solvent extraction and charcoal produced from the solid waste of olive oil press industry was used as an adsorbent for the removal of methylene blue dye from aqueous solutions (Banat et al. 2007). Batch tests showed that up to 80 % of dye was removed when the dye concentration was 10 mg/mL and the adsorbent concentration was 45 mg/mL. An increase in the olive pomace concentration resulted in greater dye removal from aqueous solution, and an increase in MB dye concentration at constant adsorbent concentration increased the dye loading per unit weight of adsorbent. The adsorption data followed the second-order kinetic model better than first order kinetic model. Charcoal showed higher adsorption capacity (uptake) than that of olive pomace. In the fixed bed adsorption experiment, the breakthrough curves showed constant pattern behavior, typical of favorable isotherms. The breakthrough time increased with increasing bed height, decreasing flow rate and decreasing influent concentration and methylene blue dye uptake. The uptake of MB dye was significantly increased when a mixture of olive pomace and charcoal was packed in the column in a multilayer fashion.

Activated carbon derived from olive waste cakes has also been employed as adsorbent for the adsorption studies of a commercial dye, Lanaset Grey G (Baccar et al. 2010). The researchers used the chemical activation method, using phosphoric acid as a dehydrating agent, for preparing the activated carbon. The BET surface area, total pore volume, and average pore diameter of the prepared activated carbon were 793 m^2/g, 0.49 cm^3/g, and 4.2 nm, respectively. At alkaline values, the pH of the metal complex dye solutions was used to study the effect of pH and no precipitation of metal hydroxides [$Co(OH)_2$ and $Cr(OH)_3$] was observed. No significant variation was observed in the amount of solute adsorbed in the pH range explored. The dye adsorption onto activated carbon prepared from olive waste cakes required an equilibrium time of 3 days, with the exterior adsorption first followed by adsorption in interior surface of the particles. The kinetics of the dye adsorption could be well understood by the adsorption primarily occurring in the boundary layer film, and then moving onto the adsorbent surface and finally diffusing into the porous structure of the adsorbent. The adsorption capacity of the activated carbon for the dye was found to be 108.7 mg/g, and the Langmuir model provided the best fit to the equilibrium data. The adsorption process followed the pseudo-first-order kinetic model and increase in temperature enhanced both rate and efficiency of the dye uptake. The dye uptake by the olive waste adsorbent was controlled by intraparticle diffusion but was not only the rate-controlling step. The adsorption process was spontaneous and endothermic in nature and the activation energy of 32.1 kJ/mol indicated that it was a physical adsorption process. In industrial solution, an adsorption capacity of 133.9 mg/g was achieved. The adsorption of a tannery dye using activated carbon prepared from olive-waste cakes was investigated (Baccar et al. 2013) and the uptake of dye was observed as 146.31 mg/g.

Phenolic compounds, pesticides, and pharmaceuticals

Phenol and substituted phenols are one of the important categories of aquatic pollutants, which are considered as toxic, hazardous, and priority pollutants. The main sources of phenol that are released into the aquatic environment are the wastewater from industries such as coke ovens in steel plants, petroleum refineries, resin, petrochemical and fertilizer, pharmaceutical, chemical, and dye industries. The removal of total phenols was investigated using several solid by-products of olive pomace processing mills (dried olive pomace, OP-1,

dried and solvent extracted olive pomace, OP-2, and dried, solvent extracted and incompletely combusted olive pomace, OP-3) (Stasinakis et al. 2008). In case of OP-1 and OP-2, the residual concentrations were higher than the initial concentration, which was attributed to the release of polyphenolic compounds contained in these adsorbents. But for OP-3, maximum phenol removal occurred in the first hour followed by a gradual attainment of equilibrium showing that only OP-3 could be used for the adsorption studies of total phenols. The pseudo-second-order model fitted well to the kinetics of total phenol removal onto OP-3. The removal of total phenols was found to increase with the increase in solution pH and maximum adsorption was achieved at pH 10.0. As the pK_a value of phenol is 9.89, it was likely that both polyphenolic compounds and surface groups coexisted in their protonated and deprotonated forms in the pH range used for the adsorption experiments. The OP-3 with particle size lower than 1.4 mm exhibited maximum adsorption capacity due to its larger surface area. Both the Langmuir and Freundlich models well explained the total phenol isotherm data. Column studies showed that decrease of influent flow rate and particle size enhanced OP-3 adsorption capacity. The adsorption capacity of OP-3 was significantly decreased after thermal or chemical regeneration (at 95 % confidence interval, using one-way ANOVA). Before regeneration, total phenols removal percentage was found to be approximately 37–38 %; however, after thermal or chemical regeneration, it remained only approximately 5–16 %. The maximum removal efficiency for total phenols was observed for thermally regenerated OP-3 at 250 °C (~14 %) and chemically regenerated OP-3 using 20 % acetone (~16 %). Activated carbon prepared from the olive husk has also been investigated as adsorbent for the removal of selected polyphenols, in particular gallic acid, p-hydroxybenzoic acid, vanillic acid, caffeic acid, and vanillin (Michailof et al. 2008). The treatment process of the olive husk involved pyrolysis, calcinations, and activation at 800 or 900 °C. Activated carbon with the highest surface area was obtained by 1 h of pyrolysis at 800 °C and activation at 800 °C for 3 h with KOH/C ratio of 4:1 (sample C2). Surface area was not altered further when the activation time was increased. Sample C5 was obtained by 1 h of pyrolysis at 800 °C and activation at 900 °C for 3 h with KOH/C ratio of 4:1 whereas sample C9 was prepared by 3 h of pyrolysis at 800 °C and activation at 900 °C for 5 h with KOH/C ratio of 4:1. These samples (C2, C5, and C9) were found to be optimum for the production of carbons with high surface area. All three carbons were found to possess more acidic groups on their surface, rather than basic ones and therefore the carbons were considered acidic. The concentration of surface phenolic and lactonic groups were found maximum in C9 and C5 carbons, respectively. The oil content of olive husk explained the acidic character of the produced carbons and the original material was held responsible for the acidic or basic nature of the final carbons rather than the activation conditions. The experiments showed that the application of prolonged pyrolysis and activation time, and high activation temperature did not influence the surface area of the produced activated carbon. But the pore size distribution was affected, and the carbons produced had wider pore distribution, with the tendency of forming mesopores and macropores. The prepared activated carbons showed good adsorption capacity for the studied pollutants as compared to commercial activated carbon. At 25 °C, the following order was noted in terms of adsorption: caffeic acid>vanillin>vanillic acid>p-hydroxybenzoic acid>gallic acid. The van der Waals forces and $\pi-\pi$ interactions were considered to control the adsorption process. Porosity was found a critical factor for the adsorption process. The carbons C2, C5, and C9 had 83, 52.5, and 76.8 % porosity, and it was observed that C2 carbon exhibited enhanced adsorption of the pollutants which was in agreement with its highly microporous nature.

Worldwide usage of pesticides has increased significantly during the last few decades and has resulted in the presence of their residues in various environmental matrices especially in groundwater and surface water. Many studies have confirmed their toxic nature to flora and fauna and their removal from water is an emerging issue. Olive stones (OS) were chemically modified and used for the removal of drin pesticides (aldrin, dieldrin, and endrin) (El Bakouri et al. 2009). The OS were dried, thermally treated at 300 °C, and then chemically treated with 1 M HCl for 8 h at room temperature to remove the ash content. The chemically and thermally activated material [acid-treated olive stone (ATOS)] was then used for pesticide adsorption tests. Thermal treatment increased the surface area of olive stones from 324 to 479 m^2/g. It also resulted in increased porosity of the treated olive stone adsorbent. The smaller the particle size, the higher was the adsorption capacity due to a substantial increase in surface area. Particles of size of 63–100 μm exhibited maximum adsorption capacity for drin pesticides. The kinetics took approximately 4 h to complete three distinct stages, first being the rapid surface adsorption followed by slow diffusion of the pesticide into the pores and finally achieved the last stage of adsorption. Pseudo-second-order model best described the adsorption of drin pesticides onto ATOS. Intraparticle diffusion was found to be the rate-controlling process. Adsorption capacity was inversely related to water-pesticide solubility and decreased in the following order: aldrin, dieldrin, and endrin. Freundlich model explained well the adsorption of pesticides onto olive stone adsorbent. The maximum multilayer adsorption capacity ranged from 3.3 to 9.7 mg/g for the studied pesticides. Weak physical forces, such as van der Waals and hydrogen bonding, were found to be responsible for the adsorption process. With the increase in temperature, a slight decrease of pesticide removal efficiency

Table 4 Adsorption capacities of olive-based adsorbents for the removal of various pollutants from water

Adsorbent	Adsorbate	Adsorbent dose	Contact time	Adsorption capacity	Temperature °C	pH	Reference
Olive stone	Pb(II)	0.5 g/50 mL	120 min	6.57 mg/g	25	5.0	(Blázquez et al. 2010)
Olive stone	Pb(II)	–	60 min	4.47×10^{-5} mol/g	20±2	5.5	(Fiol et al. 2006)
Olive stone	Pb(II)	–	–	6.66 mg/g	25	5.0	(Hernáinz et al. 2008)
Two phase olive mill solid	Pb(II)	0.5 g/50 mL	120 min	23.69 mg/g	25	5.0	(Blázquez et al. 2010)
Olive cake	Cd(II)	–	–	65.4 mg/g	28	6.0	(Al-Anber and Matouq 2008)
Succinylated-olive stone biosorbent	Cd(II)	0.5 g/L	1 h	200 mg/g	–	4.0	(Aziz et al. 2009a)
Treated olive stones	Cd(II)	–	–	128.2 mg/g	–	–	(Aziz et al. 2009b)
Olive stone	Cd(II)	–	60 min	6.88×10^{-5} mol/g	20±2	5.5	(Fiol et al. 2006)
Olive stone	Cd(II)	–	–	4.90 mg/g	25	7.0	(Hernáinz et al. 2008)
$ZnCl_2$-treated activated carbon prepared from olive stone	Cd(II)	1.0 g/50 mL	1.5 h	–	–	6.15	(Kula et al. 2008)
Olive pomace	Cd(II)	–	–	0.04 mmol/g	–	–	(Martín-Lara et al. 2008)
Olive pomace treated by H_3PO_4	Cd(II)	–	–	0.19 mmol/g	–	–	(Martín-Lara et al. 2008)
Olive pomace treated by H_2O_2	Cd(II)	–	–	0.10 mmol/g	–	–	(Martín-Lara et al. 2008)
Nonactivated waste olive cake (OCT) T=Total	Zn(II)	–	–	22 mg/g	–	–	(Fernando et al. 2009)
Non activated waste olive cake (OCP), P=>2 mm	Zn(II)	–	–	15 mg/g	–	–	(Fernando et al. 2009)
OC-HT	Zn(II)	–	–	14 mg/g	–	–	(Fernando et al. 2009)
OC-HP	Zn(II)	–	–	12 mg/g	–	–	(Fernando et al. 2009)
OC-OHT	Zn(II)	–	–	27 mg/g	–	–	(Fernando et al. 2009)
OC-OHP	Zn(II)	–	–	22 mg/g	–	–	(Fernando et al. 2009)
Olive oil mill solid residues	Zn(II)	–	60 min	5.63 mg/g	24.85	5.0	(Hawari et al. 2009)
Olive stone	Cu(II)	–	60 min	3.19×10^{-5} mol/g	20±2	5.5	(Fiol et al. 2006)
Olive pomace	Cu(II)	–		0.18 mmol/g	–	–	(Martín-Lara et al. 2008)
Olive pomace treated by H_3PO_4	Cu(II)	–	–	0.5 mmol/g	–	–	(Martín-Lara et al. 2008)
Olive pomace treated by H_2O_2	Cu(II)	–	–	0.19 mmol/g	–	–	(Martín-Lara et al. 2008)
Olive stone	Cr(III)			5.19 mg/g	25	4.0	(Blázquez et al. 2011a,b)
Olive stone	Cr(III)	–	–	6.96 mg/g	25	4.0	(Hernáinz et al. 2008)
Olive oil factory wastes	Cr(VI)	–	180 min	12.15 mg/g	25	2.0	(Malkoc et al. 2006)
Extracted olive pulp	As(III)	250 mg/25 mL	60 min	11.42 μmol/g	–	7.0	(Budinova et al. 2006)
Olive stone	As(III)	250 mg/25 mL	60 min	9.85 μmol/g	–	7.0	(Budinova et al. 2006)
Olive stone	Ni(II)	–	60 min	3.63×10^{-5} mol/g	20±2	5.5	(Fiol et al. 2006)
Olive cake	Fe(III)	–	–	–	28	4.5	(Al-Anber and Al-Anber 2008)
Activated carbon prepared by the chemical activation of olive stone	Uranium	–	5 min	0.171 mmol/g	30	6.0	(Kütahyalı and Eral 2010)
Activated carbon prepared by the chemical activation of olive stone	Thorium	–	30 min	0.087 mmol/g	30	4.0	(Kütahyalı and Eral 2010)
Treated olive stones	Safranine dye	–	–	526.3 mg/g	–	–	(Aziz et al. 2009b)
Olive husk derived activated carbons	Caffeic acid	–	–	284.59 mg/g	25	–	(Michailof et al. 2008)

Table 4 (continued)

Adsorbent	Adsorbate	Adsorbent dose	Contact time	Adsorption capacity	Temperature °C	pH	Reference
Olive husk derived activated carbons	Vanillin	–	–	191.41 mg/g	25	–	(Michailof et al. 2008)
Olive husk derived activated carbons	Vanillic acid	–	–	148.23 mg/g	25	–	(Michailof et al. 2008)
Olive husk derived activated carbons	π-hydroxybenzoic acid	–	–	101.01 mg/g	25	–	(Michailof et al. 2008)
Olive husk derived activated carbons	Gallic acid	–	–	83.84 mg/g	25	–	(Michailof et al. 2008)
Acid-treated olive stones	Aldrin	0.1 g/100 mL	4 h	9.75 mg/g	–	–	(El Bakouri et al. 2009)
Acid-treated olive stones	Dieldrin	0.1 g/100 mL	4 h	5.27 mg/g	–	–	(El Bakouri et al. 2009)
Acid-treated olive stones	Endrin	0.1 g/100 mL	4 h	3.31 mg/g	–	–	(El Bakouri et al. 2009)

was observed which was explained on the basis of solubility. The temperature increase resulted in the higher solubility of pesticide and lowered its affinity for the adsorbent surface. The adsorption of four pharmaceuticals, naproxen, diclofenac, ibuprofen, and ketoprofen on activated carbon prepared from olive-waste cakes was investigated (Baccar et al. 2012). The adsorption capacities of the carbon for the four pharmaceuticals were quite different and were linked essentially to their pK_a and their octanol/water coefficient. The adsorption kinetics of these adsorbates indicated that the adsorption process followed pseudo-second-order kinetic model for the four tested pharmaceuticals. The effect of pH and temperature on the drugs uptake by the adsorbent was also investigated. Increasing pH gradually reduced the uptake of the four pharmaceuticals, and this effect was more perceptible when the pH became alkaline.

Miscellaneous pollutants

Activated carbon (AC) prepared from olive stones and its effect on the oxidation of free cyanides by hydrogen peroxide has also been reported in literature (Yeddou et al. 2010). It was found that the presence of AC increased the reaction rate of cyanide removal. Mostly, the total removed cyanides were converted into cyanates except at the end of the test where the produced cyanates accounted for only 80 % of the removed cyanides. The kinetics of cyanide removal was well explained by pseudo-first-order model. It was observed that no toxic products were formed during the process. Besides these, several other researchers also examined the potential of olive mill solid wastes as potential adsorbents for the removal of different aquatic pollutants (Abu-El-Sha'r and Gharaibeh 1999; Aksas et al. 2012; Alaya et al. 2000; Babakhouya et al. 2010a,b; Calero et al. 2011; El-Sheikh et al. 2011; Gharaibeh et al. 1998b; Guneysu et al. 2004; Hamdaoui 2009; Khalil et al. 2000; Mameri et al. 2000; Pagnanelli et al. 2010; Pala et al. 2006; Pellera et al. 2012; Petrov et al. 2008; Román et al. 2008; Román et al. 2013; Silvestre-Albero et al. 2012; Ubago-Pérez et al. 2006; Volpe et al. 2003; Yakout and Sharaf El-Deen 2011; Yavuz et al. 2010). A comparison of various adsorbents derived from olive mill wastes for the removal of diverse types of aquatic pollutants is summarized in Table 4.

Conclusions and future prospective

In this review, an attempt has been made to focus on the recent developments related to the detoxification of water and wastewater by using olive-waste-based adsorbents. The use of waste materials as inexpensive adsorbents for removing various pollutants from water and wastewater presents many attractive features especially their contribution in the reduction of costs for waste disposal, therefore contributing to

environmental protection. Although the amount of available literature on the use of olive-waste-based adsorbents in water and wastewater treatment is increasing at a tremendous pace, there are still several gaps that need to be filled. Some of the important issues have been summarized below:

- Olive-based adsorbents have been vastly examined for metal cations removal; however, comparatively less research has been conducted on their suitability for anions and organic pollutants removal. More studies with anions and organic pollutants removal using olive-based adsorbents should be conducted.
- The physicochemical treatment conditions for the production of these adsorbents for selective and higher uptake of pollutants need to be optimized in detail.
- Composite adsorbents using olive waste (after proper treatment) should be tested for aquatic pollutants removal since such composite adsorbents might offer better performance and selective adsorption of target pollutants.
- The modified forms of olive-based adsorbents should be checked that there is no leaching of chemicals (modifying agents) in the treated water.
- Mechanistic studies need to be performed with deeper analysis to propose correct binding mechanism of aquatic pollutants with these adsorbents.
- Regeneration studies need to be performed in detail with the pollutant-laden adsorbent to recover the adsorbate as well as adsorbent. It will enhance the economic feasibility of the process.
- The potential of these adsorbents under multicomponent pollutants needs to be assessed. This would make a significant impact on the potential commercial application of olive-based adsorbents on an industrial scale.
- It is further suggested that the research should not limit to only lab-scale batch studies, but pilot-plant studies should also be conducted utilizing these adsorbents to assess their feasibility on commercial scale.
- The potential of olive-based adsorbents should also be examined for the treatment of olive oil mill wastewater since such studies are rare in literature.
- The development in the field of adsorption process using olive-based adsorbents essentially requires further investigation of testing these materials with real industrial effluents.

In conclusion, olive oil mill wastes should be seen as economic resources that can be converted into valuable products in progressing toward a permanent solution to waste disposal problems.

Acknowledgments The authors gratefully acknowledge the financial support from European Union-FP7-Regions-2009-1, STInno project (245405). Authors wish to thank all the anonymous reviewers whose comments/suggestions have significantly improved the quality of this manuscript.

References

Abu-El-Sha'r WY, Gharaibeh SH (1999) Manufacturing and environmental applications of granular activated carbon from processed solid residue of olive mill products (JEFT). Toxicol Environ Chem 68: 43–52

Ahmad T, Danish M, Rafatullah M, Ghazali A, Sulaiman O, Hashim R, Ibrahim M (2012) The use of date palm as a potential adsorbent for wastewater treatment: a review. Environ Sci Pollut Res 19:1464–1484

Aksas H, Babakhoya N, Babaci H, Feggas R, Louhab K (2012) Adsorption of chromium ions from aqueous solution using mixed sorbents prepared from olive stone and date pit. Asian J Chem 24: 4991–4994

Al-Anber ZA, Al-Anber MAS (2008) Thermodynamics and kinetic studies of iron(III) adsorption by olive cake in a batch system. J Mex Chem Soc 52:108–115

Al-Anber ZA, Matouq MAD (2008) Batch adsorption of cadmium ions from aqueous solution by means of olive cake. J Hazard Mater 151: 194–201

Al-Asheh S, Banat F (2001) Adsorption of zinc and copper ions by the solid waste of the olive oil industry. Adsorpt Sci Technol 19:117–129

Alaya MN, Hourieh MA, Youssef AM, El S, El-Sejariah F (2000) Adsorption properties of activated carbons prepared from olive stones by chemical and physical activation. Adsorpt Sci Technol 18:27–42

Amar B, Salem K, Hocine D, Chadia I, Juan MJ (2011) Study and characterization of composites materials based on polypropylene loaded with olive husk flour. J Appl Polym Sci 122:1382–1394

Arvanitoyannis IS, Kassaveti A, Stefanatos S (2007) Olive oil waste treatment: a comparative and critical presentation of methods, advantages & disadvantages. Crit Rev Food Sci Nutr 47:187–229

Attia AA, Khedr SA, Elkholy SA (2010) Adsorption of chromium ion (VI) by acid activated carbon. Braz J Chem Eng 27:183–193

Ayrilmis N, Buyuksari U (2010) Utilization of olive mill sludge in the manufacture of fiberboard. BioResources 5:1859–1867

Azbar N, Bayram A, Filibeli A, Muezzinoglu A, Sengul F, Ozer A (2004) A review of waste management options in olive oil production. Crit Rev Environ Sci Technol 34:209–247

Aziz A, Elandaloussi EH, Belhalfaoui B, Ouali MS, De Ménorval LC (2009a) Efficiency of succinylated-olive stone biosorbent on the removal of cadmium ions from aqueous solutions. Colloids Surf B Biointerfaces 73:192–198

Aziz A, Ouali MS, Elandaloussi EH, De Menorval LC, Lindheimer M (2009b) Chemically modified olive stone: a low-cost sorbent for heavy metals and basic dyes removal from aqueous solutions. J Hazard Mater 163:441–447

Babakhouya N, Aksas H, Boughrara S, Louhab K (2010a) Adsorption of Cd(II) ions from aqueous solution using mixed sorbents prepared from olive stone and date pit. J Appl Sci 10:2316–2321

Babakhouya N, Boughrara S, Abad F (2010b) Kinetics and thermodynamics of Cd(II) ions sorption on mixed sorbents prepared from olive stone and date pit from aqueous solution. Am J Environ Sci 6: 470–476

Baçaoui A, Yaacoubi A, Dahbi A, Bennouna C, Luu RPT, Maldonado-Hodar FJ, Rivera-Utrilla J, Moreno-Castilla C (2001) Optimization of conditions for the preparation of activated carbons from olive-waste cakes. Carbon 39:425–432

Baccar R, Bouzid J, Feki M, Montiel A (2009) Preparation of activated carbon from Tunisian olive-waste cakes and its application for adsorption of heavy metal ions. J Hazard Mater 162:1522–1529

Baccar R, Blánquez P, Bouzid J, Feki M, Sarrà M (2010) Equilibrium, thermodynamic and kinetic studies on adsorption of commercial dye

by activated carbon derived from olive-waste cakes. Chem Eng J 165:457–464

Baccar R, Sarrà M, Bouzid J, Feki M, Blánquez P (2012) Removal of pharmaceutical compounds by activated carbon prepared from agricultural by-product. Chem Eng J 211–212:310–317

Baccar R, Blánquez P, Bouzid J, Feki M, Attiya H, Sarrà M (2013) Modeling of adsorption isotherms and kinetics of a tannery dye onto an activated carbon prepared from an agricultural by-product. Fuel Process Technol 106:408–415

Banat F, Al-Asheh S, Al-Ahmad R, Bni-Khalid F (2007) Bench-scale and packed bed sorption of methylene blue using treated olive pomace and charcoal. Bioresour Technol 98:3017–3025

Berrios M, Martín MÁ, Martín A (2012) Treatment of pollutants in wastewater: adsorption of methylene blue onto olive-based activated carbon. J Ind Eng Chem 18:780–784

Bhatnagar A (ed.) (2012) Application of adsorbents for water pollution control. Bentham Sci Pub, Sharjah, UAE

Bhatnagar A, Sillanpää M (2009) Applications of chitin- and chitosan-derivatives for the detoxification of water and wastewater—a short review. Adv Colloid Interf Sci 152:26–38

Bhatnagar A, Sillanpää M (2010) Utilization of agro-industrial and municipal waste materials as potential adsorbents for water treatment—a review. Chem Eng J 157:277–296

Bhatnagar A, Vilar VJP, Botelho CMS, Boaventura RAR (2010) Coconut-based biosorbents for water treatment—a review of the recent literature. Adv Colloid Interf Sci 160:1–15

Blázquez G, Calero M, Hernáinz F, Tenorio G, Martín-Lara MA (2010) Equilibrium biosorption of lead(II) from aqueous solutions by solid waste from olive-oil production. Chem Eng J 160:615–622

Blázquez G, Calero M, Hernáinz F, Tenorio G, Martín-Lara MA (2011a) Batch and continuous packed column studies of chromium (III) biosorption by olive stone. Environ Prog Sustain Energy 30:576–585

Blázquez G, Martín-Lara MA, Tenorio G, Calero M (2011b) Batch biosorption of lead(II) from aqueous solutions by olive tree pruning waste: equilibrium, kinetics and thermodynamic study. Chem Eng J 168:170–177

Borja R, Raposo F, Rincòn B (2006) Treatment technologies of liquid and solid wastes from two-phase olive oil mills. Grasas Y Aceites 57:32–46

Boskou D (2006) Olive oil: chemistry and technology. American Oil Chemists Society (AOCS Press), Champaign

Budinova T, Petrov N, Razvigorova M, Parra J, Galiatsatou P (2006) Removal of arsenic(III) from aqueous solution by activated carbons prepared from solvent xxtracted olive pulp and olive stones. Ind Eng Chem Res 45:1896–1901

Calero de Hoces M, Blázquez García G, Gálvez AR, Martín-Lara MA (2010) Effect of the acid treatment of olive stone on the biosorption of lead in a packed-bed column. Ind Eng Chem Res 49:12587–12595

Calero M, Blázquez G, Martín-Lara MA (2011) Kinetic modeling of the biosorption of lead(II) from aqueous solutions by solid waste resulting from the olive oil production. J Chem Eng Data 56:3053–3060

Chuah TG, Jumasiah A, Azni I, Katayon S, Thomas Choong SY (2005) Rice husk as a potentially low-cost biosorbent for heavy metal and dye removal: an overview. Desalination 175:305–316

Cimino G, Cappello RM, Caristi C, Toscano G (2005) Characterization of carbons from olive cake by sorption of wastewater pollutants. Chemosphere 61:947–955

Crini G (2006) Non-conventional low-cost adsorbents for dye removal: a review. Bioresour Technol 97:1061–1085

DellaGreca M, Monaco P, Pinto G, Pollio A, Previtera L, Temussi F (2001) Phytotoxicity of low-molecular-weight phenols from olive mill waste waters. Bull Environ Contam Toxicol 67:0352–0359

Demiral I (2011) Methylene blue adsorption from aqueous solution using activated carbon prepared from olive bagasse. Fresenius Environ Bull 20:127–134

El Bakouri H, Usero J, Morillo J, Ouassini A (2009) Adsorptive features of acid-treated olive stones for drin pesticides: equilibrium, kinetic and thermodynamic modeling studies. Bioresour Technol 100:4147–4155

Elouear Z, Bouzid J, Boujelben N, Feki M, Montiel A (2008) The use of exhausted olive cake ash (EOCA) as a low cost adsorbent for the removal of toxic metal ions from aqueous solutions. Fuel 87:2582–2589

Elouear Z, Bouzid J, Boujelben N, Amor RB (2009) Study of adsorbent derived from exhausted olive pomace for the removal of Pb^{2+} and Zn^{2+} from aqueous solutions. Environ Eng Sci 26:767–774

El-Sheikh AH, Sweileh JA, Saleh MI (2009) Partially pyrolyzed olive pomace sorbent of high permeability for preconcentration of metals from environmental waters. J Hazard Mater 169:58–64

El-Sheikh AH, Abu Hilal MM, Sweileh JA (2011) Bio-separation, speciation and determination of chromium in water using partially pyrolyzed olive pomace sorbent. Bioresour Technol 102:5749–5756

Fernando A, Monteiro S, Pinto F, Mendes B (2009) Production of biosorbents from waste olive cake and its adsorption characteristics for Zn^{2+} ion. Sustain 1:277–297

Fiol N, Villaescusa I, Martínez M, Miralles N, Poch J, Serarols J (2006) Sorption of Pb(II), Ni(II), Cu(II) and Cd(II) from aqueous solution by olive stone waste. Sep Purif Technol 50:132–140

Galiatsatou P, Metaxas M, Kasselouri-Rigopoulou V (2002) Adsorption of zinc by activated carbons prepared from solvent extracted olive pulp. J Hazard Mater 91:187–203

Gavala HN, Skiadas IV, Ahring BK, Lyberatos G (2005) Potential for biohydrogen and methane production from olive pulp. Water Sci Technol 52:209–215

Georgieva TI, Ahring BK (2007) Potential of agroindustrial waste from olive oil industry for fuel ethanol production. Biotechnol J 2:1547–1555

Gharaibeh SH, Abu-el-sha'r WY, Al-Kofahi MM (1998a) Removal of selected heavy metals from aqueous solutions using processed solid residue of olive mill products. Water Res 32:498–502

Gharaibeh SH, Moore SV, Buck A (1998b) Effluent treatment of industrial wastewater using processed solid residue of olive mill products and commercial activated carbon. J Chem Technol Biotechnol 71:291–298

Ghazy SE, El-Morsy SM (2009) Sorption of lead from aqueous solution by modified activated carbon prepared from olive stones. Afr J Biotechnol 8:4140–4148

Guneysu S, Aydin S, Arayici S (2004) Removal of some organic acids from water using olive mill wastes as adsorbent. Fresenius Environ Bull 13:1006–1009

Hamdaoui O (2009) Removal of cadmium from aqueous medium under ultrasound assistance using olive leaves as sorbent. Chem Eng Process Process Intensif 48:1157–1166

Hamdi M (1993) Future prospects and constraints of olive mill wastewaters use and treatment: a review. Bioprocess Eng 8:209–214

Hanifi S, El-Hadrami I (2009) Olive mill wastewaters: Diversity of the fatal product in olive oil industry and its valorisation as agronomical amendment of poor soils: a review. J Agron 8:1–13

Hawari A, Rawajfih Z, Nsour N (2009) Equilibrium and thermodynamic analysis of zinc ions adsorption by olive oil mill solid residues. J Hazard Mater 168:1284–1289

Hernáinz F, Calero M, Blázquez G, Martín-Lara MA, Tenorio G (2008) Comparative study of the biosorption of cadmium(II), chromium(III), and lead(II) by olive stone. Environ Prog 27:469–478

Hodaifa G, Ochando-Pulido JM, Driss Alami SB, Rodriguez-Vives S, Martinez-Ferez A (2013) Kinetic and thermodynamic parameters of iron adsorption onto olive stones. Ind Crop Prod 49:526–534

Ihemouchen C, Djidjelli H, Boukerrou A, Fenouillot F, Barres C (2012) Effect of compatibilizing agents on the mechanical properties of high-density polyethylene/olive husk flour composites. J Appl Polymer Sci 128:2224–2229

IOC (2010) International Olive Council. http://www.internationaloliveoil.org/

Khalil L, Girgis B, Tawfik T (2000) Porosity characteristics of activated carbons derived from olive oil wastes impregnated with H_3PO_4. Adsorpt Sci Technol 18:373–383

Konstantinou M, Pashalidis I (2007) Adsorption of hexavalent uranium on biomass by-product. J Radioanal Nuclear Chem 273:549–552

Konstantinou M, Kolokassidou K, Pashalidis I (2007) Sorption of Cu(II) and Eu(III) ions from aqueous solution by olive cake. Adsorption 13:33–40

Kula I, Uğurlu M, Karaoğlu H, Çelik A (2008) Adsorption of Cd(II) ions from aqueous solutions using activated carbon prepared from olive stone by $ZnCl_2$ activation. Bioresour Technol 99:492–501

Kütahyalı C, Eral M (2010) Sorption studies of uranium and thorium on activated carbon prepared from olive stones: kinetic and thermodynamic aspects. J Nucl Mater 396:251–256

La Rubia-García MD, Yebra-Rodríguez Á, Eliche-Quesada D, Corpas-Iglesias FA, López-Galindo A (2012) Assessment of olive mill solid residue (pomace) as an additive in lightweight brick production. Constr Build Mater 36:495–500

Lucey MR (2002) Olive mill solid residues as heavy metal sorbent material: a preliminary study. Waste Manage 22:901–907

Malkoc E, Nuhoglu Y, Dundar M (2006) Adsorption of chromium(VI) on pomace—an olive oil industry waste: batch and column studies. J Hazard Mater 138:142–151

Mameri N, Aioueche F, Belhocine D, Grib H, Lounici H, Piron DL, Yahiat Y (2000) Preparation of activated carbon from olive mill solid residue. J Chem Technol Biotechnol 75:625–631

Mantzavinos D, Kalogerakis N (2005) Treatment of olive mill effluents: Part I. Organic matter degradation by chemical and biological processes—an overview. Environ Int 31:289–295

Martinez-Garcia G, Bachmann RT, Williams CJ, Burgoyne A, Edyvean RGJ (2006) Olive oil waste as a biosorbent for heavy metals. Int Biodeterior Biodegrad 58:231–238

Martín-Lara MA, Pagnanelli F, Mainelli S, Calero M, Toro L (2008) Chemical treatment of olive pomace: effect on acid-basic properties and metal biosorption capacity. J Hazard Mater 156:448–457

Martín-Lara MA, Hernáinz F, Calero M, Blázquez G, Tenorio G (2009) Surface chemistry evaluation of some solid wastes from olive-oil industry used for lead removal from aqueous solutions. Biochem Eng J 44:151–159

Martín-Lara MA, Rodríguez IL, Blázquez G, Calero M (2011) Factorial experimental design for optimizating the removal conditions of lead ions from aqueous solutions by three wastes of the olive-oil production. Desalination 278:132–140

Metaxas M, Kasselouri-Rigopoulou V, Galiatsatou P, Konstantopoulou C, Oikonomou D (2003) Thorium removal by different adsorbents. J Hazard Mater 97:71–82

Michailof C, Stavropoulos GG, Panayiotou C (2008) Enhanced adsorption of phenolic compounds, commonly encountered in olive mill wastewaters, on olive husk derived activated carbons. Bioresour Technol 99:6400–6408

Moftah O, Grbavčić S, Žuža M, Luković N, Bezbradica D, Knežević-Jugović Z (2012) Adding value to the oil cake as a waste from oil processing industry: production of lipase and protease by *Candida utilis* in solid state fermentation. Appl Biochem Biotech 166:348–364

Mousa A, Heinrich G, Gohs U, Hässler R, Wagenknecht U (2009) Application of renewable agro-waste-based olive pomace on the mechanical and thermal performance of toughened PVC. Polymer Plast Technol Eng 48:1030–1040

Nefzaoui (1995) Olive by-products recycling. Proc. of the International Symposium on olive oil processes and by-products recycling, Granada

Niaounakis M, Halvadakis CP (2006) Olive processing waste management—literature review and patent survey, 2nd edn. Elsevier, Oxford UK

Nieto LM, Alami SBD, Hodaifa G, Faur C, Rodríguez S, Giménez JA, Ochando J (2010) Adsorption of iron on crude olive stones. Ind Crop Prod 32:467–471

Nuhoglu Y, Malkoc E (2009) Thermodynamic and kinetic studies for environmentaly friendly Ni(II) biosorption using waste pomace of olive oil factory. Bioresour Technol 100:2375–2380

Pagnanelli F, Toro L, Vegliò F (2002) Olive mill solid residues as heavy metal sorbent material: a preliminary study. Waste Manage 22:901–907

Pagnanelli F, Mainelli S, Vegliò F, Toro L (2003) Heavy metal removal by olive pomace: biosorbent characterisation and equilibrium modelling. Chem Eng Sci 58:4709–4717

Pagnanelli F, Viggi CC, Toro L (2010) Development of new composite biosorbents from olive pomace wastes. Appl Surf Sci 256:5492–5497

Pala A, Galiatsatou P, Tokat E, Erkaya H, Israilides C, Arapoglou D (2006) The use of activated carbon from olive oil mill residue, for the removal of colour from textile wastewater. Eur Water 13(14):29–34

Paraskeva P, Diamadopoulos E (2006) Technologies for olive mill wastewater (OMW) treatment: a review. J Chem Technol Biotechnol 81: 1475–1485

Paraskeva CA, Papadakis VG, Kanellopoulou DG, Koutsoukos PG, Angelopoulos KC (2007a) Membrane filtration of olive mill wastewater and exploitation of its fractions. Water Environ Res 79:421–429

Paraskeva CA, Papadakis VG, Tsarouchi E, Kanellopoulou DG, Koutsoukos PG (2007b) Membrane processing for olive mill wastewater fractionation. Desalination 213:218–229

Paredes MJ, Moreno E, Ramos-Cormenzana A, Martinez J (1987) Characteristics of soil after pollution with waste waters from olive oil extraction plants. Chemosphere 16:1557–1564

Pellera F-M, Giannis A, Kalderis D, Anastasiadou K, Stegmann R, Wang J-Y, Gidarakos E (2012) Adsorption of Cu(II) ions from aqueous solutions on biochars prepared from agricultural by-products. J Environ Manage 96:35–42

Pereira M, Arroyo P, de Barros M, Sanches V, da Silva E, Fonseca I, Lovera R (2006) Chromium adsorption in olive stone activated carbon. Adsorption 12:155–162

Petrov N, Budinova T, Razvigorova M, Parra J, Galiatsatou P (2008) Conversion of olive wastes to volatiles and carbon adsorbents. Biomass Bioenergy 32:1303–1310

Pirrone N, Keeler GJ, Nriagu JO (1996) Regional differences in worldwide emissions of mercury to the atmosphere. Atmos Environ 30: 2981–2987

Rana G, Rinaldi M, Introna M (2003) Volatilisation of substances alter spreading olive oil waste water on the soil in a Mediterranean environment. Agric Ecosyst Environ 96:49–58

Roig A, Cayuela ML, Sánchez-Monedero MA (2006) An overview on olive mill wastes and their valorisation methods. Waste Manag 26: 960–969

Román S, González JF, González-García CM, Zamora F (2008) Control of pore development during CO_2 and steam activation of olive stones. Fuel Process Technol 89:715–720

Román S, Valente Nabais JM, Ledesma B, González JF, Laginhas C, Titirici MM (2013) Production of low-cost adsorbents with tunable surface chemistry by conjunction of hydrothermal carbonization and activation processes. Microporous Mesoporous Mater 165:127–133

Rouibah K, Meniai A-H, Rouibah MT, Deffous L, Lehocine MB (2009) Elimination of chromium (VI) and cadmium(II) from aqueous solutions by adsorption onto olive stones. The Open Chem Eng J 3:41–48

Rouibah K, Meniai AH, Deffous L, Lehocine MB (2010) Chromium VI and cadmium II removal from aqueous solutions by olive stones. Desalin Water Treat 16:393–401

Schwarzenbach RP, Escher BI, Fenner K, Hofstetter TB, Johnson CA, von Gunten U, Wehrli B (2006) The challenge of micropollutants in aquatic systems. Science 313:1072–1077

Sesli M, Yeğenoğlu ED (2009) RAPD-PCR analysis of cultured type olives in Turkey. Afr J Biotechnol 8:3418–3423

Silvestre-Albero J, Silvestre-Albero A, Rodríguez-Reinoso F, Thommes M (2012) Physical characterization of activated carbons with narrow microporosity by nitrogen (77.4K), carbon dioxide (273K) and argon (87.3K) adsorption in combination with immersion calorimetry. Carbon 50:3128–3133

Siracusa G, La Rosa AD, Siracusa V, Trovato M (2001) Eco-compatible use of olive husk as filler in thermoplastic composites. J Polym Environ 9:157–161

Spahis N, Addoun A, Mahmoudi H, Ghaffour N (2008) Purification of water by activated carbon prepared from olive stones. Desalination 222:519–527

Stamatakis G (2010) Energy and geo-environmental applications for olive mill wastes. a review. Hellenic J Geosci 45:269–282

Stasinakis AS, Elia I, Petalas AV, Halvadakis CP (2008) Removal of total phenols from olive-mill wastewater using an agricultural by-product, olive pomace. J Hazard Mater 160:408–413

Ubago-Pérez R, Carrasco-Marín F, Fairén-Jiménez D, Moreno-Castilla C (2006) Granular and monolithic activated carbons from KOH-activation of olive stones. Microporous Mesoporous Mater 92:64–70

Uğurlu M, Gürses A, Doğar Ç (2007) Adsorption studies on the treatment of textile dyeing effluent by activated carbon prepared from olive stone by $ZnCl_2$ activation. Color Technol 123:106–114

Uğurlu M, Gürses A, Açıkyıldız M (2008) Comparison of textile dyeing effluent adsorption on commercial activated carbon and activated carbon prepared from olive stone by $ZnCl_2$ activation. Microporous Mesoporous Mater 111:228–235

Uğurlu M, Kula I, Karaoğlu MH, Arslan Y (2009) Removal of Ni(II) ions from aqueous solutions using activated-carbon prepared from olive stone by $ZnCl_2$ activation. Environ Prog Sust Energ 28:547–557

UNESCO (2003) World Water Assessment Programme, Water for People, Water for Life—the United Nations World Water Development Report

Uzunosmanoglu O, Uyanik A, Engin MS (2011) The removal of cadmium (II), copper (II) and lead (II) from aqueous solutions by olive tree pruning waste. Fresenius Environ Bull 20:3135–3140

Vegliò F, Beolchini F, Prisciandaro M (2003) Sorption of copper by olive mill residues. Water Res 37:4895–4903

Volpe A, Lopez A, Pagano M (2003) Olive husk: an alternative sorbent for removing heavy metals from aqueous streams. Appl Biochem Biotechnol 110:137–149

Wahby A, Abdelouahab-Reddam Z, El Mail R, Stitou M, Silvestre-Albero J, Sepúlveda-Escribano A, Rodríguez-Reinoso F (2011) Mercury removal from aqueous solution by adsorption on activated carbons prepared from olive stones. Adsorption 17:603–609

Wang Q, Kim D, Dionysiou DD, Sorial GA, Timberlake D (2004) Sources and remediation for mercury contamination in aquatic systems—a literature review. Environ Pollut 131:323–336

Yakout SM, Sharaf El-Deen G (2011) Characterization of activated carbon prepared by phosphoric acid activation of olive stones. Arabian J Chem. doi:10.1016/j.arabjc.2011.12.002

Yavuz R, Akyildiz H, Karatepe N, Çetinkaya E (2010) Influence of preparation conditions on porous structures of olive stone activated by H_3PO_4. Fuel Process Technol 91:80–87

Yeddou AR, Nadjemi B, Halet F, Ould-Dris A, Capart R (2010) Removal of cyanide in aqueous solution by oxidation with hydrogen peroxide in presence of activated carbon prepared from olive stones. Miner Eng 23:32–39

Zervakis G, Balis C (1996) Bioremediation of olive oil mill wastes through the production of fungal biomass In: Royse (Hrsg.), Mushroom biology and mushroom products. Proceedings of the 2nd International Conference. Penn State Univ., University Park

Zhou Y-F, Haynes RJ (2010) Sorption of heavy metals by inorganic and organic components of solid wastes: significance to use of wastes as low-cost adsorbents and immobilizing agents. Crit Rev Environ Sci Technol 40:909–977